Molecular analysis of the early interaction between the grapevine flower and Botrytis cinerea reveals that prompt activation of specific host pathways leads to fungus quiescence.

Title: Molecular analysis of the early interaction between the grapevine flower and *Botrytis cinerea* reveals that prompt activation of specific host pathways leads to fungus quiescence.

Running Title: *Vitis vinifera* flower and *Botrytis cinerea* quiescence

Short summary: A rapid defense response of the grapevine flower to *Botrytis cinerea*, based on the activation of stilbenoid and ROS metabolism and cell wall reinforcement, leads to fungus quiescence.

Zeraye H. Mehari[1,6], Stefania Pilati[1], Paolo Sonego[2], Giulia Malacarne[1], Urska Vrhovsek[3], Kristof Engelen[2], Paul Tudzynski[4], Michela Zottini[5], Elena Baraldi[6], Claudio Moser[1*]

[1]Genomics and Biology of Fruit Crops Department, Research and Innovation Centre, Fondazione Edmund Mach, Via E. Mach 1, San Michele all'Adige 38010 (TN), Italy.

[2]Computational Biology Department, Research and Innovation Centre, Fondazione Edmund Mach, Via E. Mach 1, San Michele all'Adige 38010 (TN), Italy.

[3]Food Quality and Nutrition Department, Research and Innovation Centre, Fondazione Edmund Mach, Via E. Mach 1, San Michele all'Adige 38010 (TN), Italy.

[4]Institute for biology and biotechnology of plants Westf. Wilhelms University, Schlossplatz 8 D-48143 Muenster, Germany.

[5]Department of Biology, University of Padua, Italy, Via U. Bassi 58/B, 35131 Padua, Italy

[6]Department of Agricultural Sciences, University of Bologna, Viale Fanin, 46, 40127, Bologna

*** Corresponding author: Claudio Moser** (claudio.moser@fmach.it)

Principal investigator, Ph.D

Department of Genomics and Biology of Fruit Crops, Research and Innovation Centre, Fondazione Edmund Mach (FEM), San Michele all'Adige (TN), Italy.

ABSTRACT

Grapes quality and yield can be impaired by bunch rot, caused by the necrotrophic fungus *Botrytis cinerea*. Infection often occurs at flowering and the pathogen stays quiescent until fruit maturity. Here, we report a molecular analysis of the early interaction between *B. cinerea* and *Vitis vinifera* flowers, using a controlled infection system, confocal microscopy and integrated transcriptomic and metabolic analysis of the host and the pathogen. Flowers from fruiting cuttings of the cv. Pinot Noir were infected with GFP-labeled *B. cinerea* and studied at 24 and 96 hours post inoculation (hpi). We observed that penetration of the epidermis by *B. cinerea* coincided with increased expression of genes encoding cell wall-degrading enzymes, phytotoxins, and proteases. Grapevine responded with a rapid defense reaction involving 1193 genes associated with the accumulation of antimicrobial proteins, polyphenols, reactive oxygen species and cell wall reinforcement. At 96 hpi the reaction appears largely diminished both in the host and in the pathogen. Our data indicate that the defense responses of the grapevine flower collectively are able to restrict invasive fungal growth into the underlying tissues, thereby forcing the fungus to enter quiescence until the conditions become more favorable to resume pathogenic development.

Key words: *Vitis vinifera*, *Botrytis cinerea*, quiescence, defence response.

INTRODUCTION

Grapevine yield and quality faces challenges worldwide from biotic stresses, mainly caused by fungi and oomycetes like *Botrytis cinerea*, *Plasmopara viticola*, and *Erysiphe necator*. *B. cinerea*, a necrotroph responsible for pre- and post-harvest disease in many crops, causes bunch rot in grapevine. In vineyards, *B. cinerea* is part of the natural microflora where primary infections of berries are usually initiated by airborne conidia from overwintering sources (Nair *et al*. 1995; Elmer & Michailides 2004). Bunch rot frequently occurs on ripe berries close to harvest. Wet conditions together with damage to ripe berries, due to cuticle cracking from pressure within the berry/cluster and physical damage occurring during ripening, cause the expression of bunch rot, even though the primary infection could have occurred at earlier stages of berry development (McClellan & Hewitt 1973; Nair *et al*. 1995). Bunches inoculated at flowering were reported to have higher disease severity at maturity (Keller *et al*. 2003; Pezet *et al*. 2003b), implying that bunch rot disease observed during ripening may not only be due to *de novo* infection, but also due to latent infections that occurred at earlier stages of berry development. A similar infection strategy of the pathogen was also observed in strawberries and raspberries (Jarvis 1962; Williamson *et al*. 1987; Jersch *et al*. 1989). This delayed asymptomatic infection is known as quiescent infection.

Usually *B. cinerea*, upon contact with the host, incites cell death by producing phytotoxins and cell wall-degrading enzymes and manipulates host metabolism to facilitate colonization (van Kan 2006; Choquer *et al*. 2007; Williamson *et al*. 2007). A deviation from this common necrotrophic lifestyle, where *B. cinerea* behaves as a facultative endophyte has also been reported (Williamson *et al*.1987; McNicol & Williamson 1989; Coertze & Holz 2002; van Kan et al., 2014; Shaw *et al*. 2016).

In grapevine, *B*. *cinerea* infection often occurs at blooming and then remains quiescent until ripening (McClellan & Hewitt 1973; Nair *et al*. 1995; Keller *et al*. 2003; Pezet *et al*. 2003b). Berry developmental stages between bloom and véraison are mostly resistant to *B*. *cinerea* infection. Such development related resistance could be linked to preformed and inducible antifungal compounds, as well as skin features of immature berries. Phenylpropanoid and flavonoid extracts of young berries, as well as resveratrol, can inhibit *B*. *cinerea* growth (Goetz *et al*.1999; Schouten *et al*. 2002b; Pezet *et al*. 2003b). Furthermore, polyphenols in the berry skin cell wall and the thickness of epidermal cell layer complex were reported among the resistance factors (Mlikota-Gabler *et al*. 2003; Deytieux-Belleau *et al*. 2009). More recently, Agudelo-Romero et al. (2015) reported a large transcriptional activation of genes related to secondary metabolism and hormonal signaling (jasmonic acid [JA], ethylene [ET], and auxins) upon *B*. *cinerea* infection of immature berries of cv. Trincadeira. Another study on grapes infected at véraison reported the accumulation of reactive oxygen species (ROS), the activation of the salicylic acid (SA) dependent pathway and the induction of stilbene and lignin biosynthesis as defense mechanisms to arrest *B*. *cinerea* progression (Kelloniemi *et al*. 2015).

In disease management, quiescent infection has important implications for proper timing of prophylactic measures, to reduce stress factors that may trigger egression of the quiescent pathogen, and to prolong quiescence to the point where the produce is not affected even after harvest (Jarvis 1994). Concerning grapevine, flowering is an important stage in the epidemiology of *B*. *cinerea* as infection at this stage is followed by quiescence. Therefore, understanding the interaction between *B*. *cinerea* and grapevine inflorescence is vital to implement proper management in order to limit consequent yield losses. Despite this, knowledge about the molecular mechanisms of the interplay between *B*. *cinerea* and grapevine inflorescences at bloom is lacking. Taking advantage of the availability of the

genome sequences of *Vitis vinifera* (Jaillon et al. 2007; Velasco *et al*. 2007) and *B*. *cinerea* (Amselem *et al*. 2011; van Kan *et al*. 2016), we analyzed the transcriptional alterations of both organisms during flower infection to understand the molecular mechanisms associated with the early stage of this interaction. Microscopic observation and metabolic profiles were combined with the transcriptomic analyses to further our understanding of the infection process at infection initiation and initial fungal quiescent stages.

MATERIALS AND METHODS

Plant material and *B*. *cinerea* inoculation

Winter woody cuttings were collected from an experimental vineyard (*Vitis vinifera* cv. Pinot Noir) of the Fondazione Edmund Mach, Trentino-Alto Adige, Italy and stored at 4 °C until use. Flowers were raised from the cuttings following the technique of Mullins and Rajaskekaren (1981). At EL17, according to Eichorn & Lorenz (1977), flowers were thinned to ensure that each flower could receive *B*. *cinerea* conidia. Cuttings were grown in a growth chamber at 24°C, with a 16 h light cycle.

Transgenic *V*. *vinifera* plants (Microvine mutant) harboring the H_2O_2-specific HyPer probe, targeted to the cytosol, were generated as described in Costa *el al*. (2010).

Botrytis cinerea (isolate B05.10) was cultured on potato dextrose agar (PDA, in Petri dishes) at 25 °C. After 10 days, conidia were harvested in distilled water and filtered with sterile pippet tip plugged with cotton wool. The concentration was determined using a hemacytometer. At full cap-fall stage (EL25/26), each flower was inoculated by positioning 1.5 µl of a $2*10^5$ ml^{-1} conidia solution close to receptacle area (Supporting Information Fig. S1). After inoculation, the whole cutting was bagged in water sprayed, clear plastic bag for 24 h to ensure high humidity, an essential factor for conidial germination.

For microscopic observation and post-inoculation evaluation (plating out test), a B05.10 transformant expressing a codon-optimized green fluorescent protein (GFP) (Leroch et al. 2011) under control of the constitutive oliC promoter from *Aspergillus nidulans*, named PoliC::GFP (Schumacher 2012), was used due to its fluorescent signal and ability to grow on selective medium (PDA with70 µg/ml Hygromycin B). The.construct is integrated at the bcniiA locus, and the strain is homokaryotic.

Microscopic observations and detection of quiescent *B. cinerea*

Confocal laser scanning microscopy analyses were performed using a Leica SP5 imaging system (Leica Microsystems, Germany) and a Zeiss LSM700 (Carl Zeiss Microscopy, Germany). GFP and chlorophyll were excited at 488 nm and the emission was collected at 515-560 nm and 650-750 nm, respectively. For HyPer detection confocal microscopy analyses were performed according to Costa *et al*. (2010). Thin slices, which were manually cut from inoculated flowers, were subjected to microscopic observation.

For quiescent *B*. *cinerea* detection, the plating out method on selective medium was used. Eight fruitlets from each of 6 biological replicates were sampled daily from 1 to 7 and at 14 days post inoculation were incubated on selective medium at room temperature for a week before or after washing, or after surface sterilization. Washing was with sterile water, three rinses of 1 minute each with gentle shaking; whereas surface sterilization was carried out with 70% ethanol (1 min) followed by 1% (vol/vol) NaClO (3 min) and three rinses in sterile water (Keller *et al*. 2003). Appearance of mycelial growth was scored as confirmation of quiescent *B*. *cinerea* on the fruitlets. Fruitlets > 4 mm in diameter (approximately) were cut into half before plating. Statistical significance was calculated by Tukey's Honestly Significant Difference test on square root transformed data.

Secondary metabolites and RNA extraction

Inflorescences from fruiting cuttings that were either mock or B05.10-conidia inoculated at cap-off stage, were collected at 12, 24, 48, 72 and 96 hpi, in three biological replicates, immediately frozen in liquid nitrogen and kept at -80 °C until use. An inflorescence from a fruiting cutting was considered as a biological replicate. RNA was extracted using Plant Total RNA Kit (Sigma-Aldrich) following the manufacturer's protocol. For polyphenol analysis, sample preparation and Ultra High Performance Liquid Chromatography - Diode Array Detection - Mass Spectrometry (UHPLC-DAD-MS) analysis were conducted as described in Vrhovsek *et al*. (2012). The samples used for polyphenol and RNA extraction were independent.

For *B*. *cinerea* RNA extraction, B05.10 conidia were incubated in flask with PDB for 12 h (Supporting Information Fig. S2) with 30 rpm shake in three biological replicates. Conidia obtained from a Petri dish were considered as a biological replicate.

RNA sequencing, data processing and data analysis

Samples collected at 24 and 96 hpi were used for RNA-Seq analysis. Approximately 20 million strand-specific, 100 bp long sequences, were obtained for each sample using a Next Generation Sequencing Platform HiSeq 1500 (Illumina, San Diego, CA). The quality of the the Illumina single-end reads was checked using FastQC (version 0.11.2) (http://www.bioinformatics.babraham.ac.uk/projects/fastqc/) and pre-processed for adapter with cutadapt (version 1.8.1) (Martin, 2011). The resulting reads were aligned separately to the *B.cinerea* (strain B05.10) (http://fungi.ensembl.org) and the grapevine (12Xv1, http://genomes.cribi.unipd.it/) genomes using Subread aligner (Liao *et al*. 2013). Raw read counts were extracted from the Subread alignments using featureCount read summarization program (Liao *et al*. 2014). All raw RNA-Seq read data are deposited in the NCBI Short Read

Archive (http://www.ncbi.nlm.nih.gov/sra/) under the BioProject accession code PRJNA336478 and SRA accession code SRP080917.

Differential expression analysis was performed after the mean-variance relationship of the log-counts was computed using voom method (Law *et al*. 2014), which generates a precision weight for each observation to feed to the limma empirical Bayes analysis pipeline (Smyth 2004). Genes were considered differentially expressed if they fulfill a *p*-value <0.05 and an absolute fold change of ≥1.5. Gene ontology enrichment was computed using customized annotation and annotated reference into the AgriGO analysis tool (http://bioinfo.cau.edu.cn/agriGO/analysis.php; Du Z *et al*. 2010). Enriched molecular networks ($P < 0.05$) were identified using VESPUCCI (http://vespucci.colombos.fmach.it) (Moretto *et al*. 2016) based on VitisNet annotation (Grimplet *et al*. 2012). MapMan tool (Thimm *et al*. 2004) was used to visualize differentially expressed genes in the context of biotic stress pathway using the GrapeGen 12Xv1 annotations version (Lijavetzky *et al*. 2012) as MapMan Bins.

Quantitative polymerase chain reaction (qPCR)

cDNA was synthesized from 3 µg of the same RNA used for RNA-Seq analysis, treated with DNase I (Ambion), using the SuperScript™VILO™cDNA Synthesis Kit (Invitrogen). qPCR was performed in a Viia7 thermocycler (Applied Biosytems) using 0.31 µl of cDNA and 2.5 µM of primers in a total volume of 12.5 µl where half of the total volume was Fast SYBR Green Master Mix (Kapa Biosystems). Each amplification reaction was run in triplicate. For normalization, *VvACT* and *VvTUB*, and *BcRPL5* and *BcTUBA* genes were selected using GeNORM (Vandesompele *et al*. 2002) as reference for grapevine and *B*. *cinerea*, respectively. Amplification efficiencies of each primer pair were calculated with LinReg (Ruijter *et al*. 2009). The obtained amplification efficiency was used to calculate the relative quantity (RQ) and normalized relative quantity (NRQ) according to Hellemans *et al*. (2007).

Statistical analyses of the qPCR results were made after $\log_2$(NRQ) transformation (Rieu and Powers 2009). All primers and corresponding gene identifiers can be found in Supporting Information Data S1. Statistical significance was calculated by Tukey's Honestly Significant Difference test or an unpaired heteroscedastic Student's *t* test, considering each technical replicate as an individual sample.

DNA extraction, standard curve and DNA quantification

DNA was isolated from grapevine flowers and *B. cinerea* (strain B05.10) mycelium, obtained from conidia incubated for 48 h as mentioned above, using the Dneasy Plant Minikit (Qiagen) following the manufacturer's protocol. DNA from mycelium and uninoculated grapevine flower were used to generate calibration curves to estimate the amount of fungal DNA in inoculated samples. Samples were replicated three times.

Genomic DNA was used as a template for qPCR using primers *Bc3*, ribosomal IGS spacer, and *VvRS I*, resveratrol synthase gene I, with similar amplification procedure described above. For the standard curve, qPCR reaction were carried out in triplicate from known fungal or plant DNA extracts which were serially diluted 5 times. The standard curves were generated by plotting the log of DNA (pg) against the Ct value (Supporting Information Fig. S3). The Ct values obtained from inoculated samples were used to extrapolate the amount of genomic DNA from the standard curves. Genomic DNA of *B. cinerea* in a sample was normalized to the amount of grapevine genomic DNA in that sample.

RESULTS

***Botrytis cinerea* infection of grapevine flower**

Artificial infection of grapevine flowers with GFP-labeled B05.10 strain was conducted at full cap-off stage (EL25/26) (Figure 1A). The infection was monitored for two weeks post inoculation (wpi) and during this period there were no visible symptoms of infection or fungal growth (Figure 1B-E). Although fungal conidia germination, formation of appressoria

and penetration into the flower cuticle on the gynoecium were observed 24 hours post inoculation (hpi) (Figure 1F and Supporting Information Fig. S4), no substantial growth progress was appreciated at 96 hpi (Figure 1G). The presence of viable fungus during 2 wpi was confirmed by plating out experiments. Inoculated but healthy-looking fruitlets were incubated on selective media to allow the growth of the GFP-labeled *Botrytis* strain only. Germinated *B*. *cinerea* conidia were present on the skin of 90 % of the inoculated fruitlets, whereas about 30 % of the samples showed the presence of *B*. *cinerea* below the external cell layers of the fruitlet (Figure 1H). A preliminary test confirmed that washing within 6 hpi was able to remove ungerminated conidia from flowers and that surface sterilization abolished *B*. *cinerea* viability (Supporting Information Fig. S5).

To check if a similar load of *B*. *cinerea* was present at different post inoculation times, the amount of fungal and grapevine DNA was estimated by quantifying *Bc3* and *VvRS I* genes, respectively (Supporting Information Fig. S3A-B). As shown in Figure 2A, the relative amount of fungal DNA compared to plant DNA ranged from 4 to 6%, with a slight increase within two dpi, indicating initial pathogen growth, followed by a slight decrease possibly associated to a quiescent state. Furthermore, the expression profile of *B*. *cinerea* actin, an indicator of active growth, confirmed that the growth of the fungus was relatively high up to two dpi, and then decreased slightly but significantly, supporting pathogen quiescence (Figure 2B).

Inoculated inflorescences were inspected until ripening. At full coloring (approximately 10 wpi), bunches were either bagged with plastic bags, to create favorable humidity for *B*. *cinerea*, or left as such. Two weeks after bagging, egression of *B*. *cinerea* was observed on about 40 % of the inoculated berries (Supporting Information Fig. S6A). Cross checking of the fungal strain, using fluorescence microscope, confirmed that it was the GFP-labeled B05.10 strain inoculated at cap-off stage (Supporting Information Fig. S6B). On the other

hand, no egression was observed from unbagged bunches. To see if bagging can trigger egression before maturity, bunches at pepper-corn stage, which were infected at cap-off stage, were bagged for two weeks, but no egression was observed (Supporting Information Fig. S7).

Transcriptome analysis of infected grapevine flowers

Three biological replicates of mock or B05.10 inoculated flowers were harvested at 24 and 96 hpi for dual (plant and fungus) RNA-seq analysis. These time points were chosen to understand the process of infection initiation (24 hpi) and progress (96 hpi), if any. The fraction of reads from *Botrytis*- and mock-inoculated flowers mapped to the grapevine reference genome was between 65 and 82 %, whereas only up to 4.6 % could be mapped to the *B. cinerea* genome (Supporting Information Data S2). In the case of *B. cinerea*, cultured in potato dextrose broth (PDB), used as control sample, about 90 % of reads was mapped to the fungal genome, suggesting that the scarce number of fungus reads derived from the infected flowers is likely caused by low number of conidia used for the infection (around 300) and of the limited fungal growth after inoculation.

As for grapevine, the biological variability within replicates and among experimental conditions was analyzed by principal component analysis (PCA). As shown in Figure 3A, the first principal component separates the two time-points (24 and 96 hpi) and also the 24-hours' *Botrytis* treated vs. untreated samples. In contrast, all samples collected at 96 hpi seem very similar at a whole transcriptome level, as indicated by the large overlap in the PCA.

Differential expression of grapevine genes was calculated between *Botrytis*- vs. mock-inoculated flowers (Supporting Information Data S3) within each time point. At 24 hpi, 1193 genes were differentially expressed (upregulated or downregulated), whereas at 96 hpi only 265 genes were differentially expressed (Figure 3B, Supporting Information Fig. S8 and Supporting Information Data S4). The overlap between the two sets was limited to 49

upregulated and 4 downregulated genes (Figure 3C). Interestingly, at 24 hpi the plant seems to respond to the presence of the pathogen with a prevalent induction of genes, which appeared to be no longer modulated at 96 hpi.

Gene expression values from RNA-Seq analysis were validated using qPCR assay. The expression measurement of 20 grapevine genes (Supporting Information Data S5) by qPCR was in very good agreement (R^2 >0.90) with the results obtained by RNA-Seq (Figure 3D).

Defense related responses are largely induced in the flower upon *B. cinerea* infection

Differentially expressed (DE) genes were annotated according to Gene Ontology (GO) (http://genomes.cribi.unipd.it/grape/) and VitisNet (https://www.sdstate.edu/ps/research/vitis/pathways.cfm) databases. GO functional class enrichment and VitisNet analysis provided consistent and complementary results (Table 1 and Supporting Information Data S6). A clear regulation of those classes typically modulated during biotic stress responses was found, as depicted in the MapMan pathway (Figure 4), and in the enriched set of *Botrytis*-infected flowers (Supporting Information Data S7). In the following text, these classes are presented in detail.

One of the earliest cellular responses following plant-pathogen interaction is the production of reactive oxygen species (ROS). Upon *B. cinerea* infection, genes encoding enzymes involved in oxidative stress such as GST, ascorbate oxidase, 2OG-Fe(II) oxygenase, and cytochrome P450 monooxygenases were strongly upregulated (Table 2 and Supporting Information Data S8). ROS accumulation at 24 hpi was proven by a localized green fluorescence emitted at the site of penetration in flowers obtained from a cytoplasmic HyPer (cHyPer) transgenic line (Figure 5).

Several genes encoding membrane-localized receptor-like kinases (*RLK*), such as, *CLV1*, *WAK1*, and *BAK1*, which have been characterized in connection with immune responses to necrotrophic pathogens (Kemmerling *et al*. 2007; Brutus *et al*. 2010), were also upregulated at 24 hpi (Supporting Information Data S8). Genes associated with phytohormones, known to be involved in pathogen response signaling, were also differentially expressed (Figure 4 and Table 1). According to the number of DE genes related to ET biosynthesis or signaling, this hormone seems to be important in the interaction between grapevine flower and *B*. *cinerea*. Two *ACC synthase* and one *ACC oxidase* genes in addition to seven ET responsive TFs were differentially expressed (Supporting Information Data S8). Also genes encoding an SA marker *PR1* and the plant defense regulator involving SA signaling *EDS1* (Wiermer *et al*. 2005) were upregulated in the infected sample at 24 hpi (Table 2). Jasmonate ZIM-domain gene, a marker for JA, was also upregulated. Other genes involved in the synthesis of and signalling by phytohormones (apart from ET, JA and SA pathways) showed changes in transcript levels following inoculation with *B*. *cinerea*, suggesting a complex hormonal interplay. For example, five genes encoding nitrilase and nitrile hydratases, involved in indole 3-acetic acid synthesis, were differentially regulated, as well as receptor genes for gibberellic acid (GA) and abscisic acid (ABA) (Supplemetal Data S2). The global hormonal alterations related to infection were evaluated by Hormonometer software (Volodarsky *et al*. 2009), which also suggested the involvement of several hormones (Supporting Information Fig. S9).

Following the *Botrytis*-induced signaling cascades, about 100 transcription factors (TF) were differentially expressed in infected flowers. Most prominent were genes encoding WRKY, MYB, ethylene-responsive element-binding proteins, and NAC TFs (Supporting Information Data S8). Among the transcriptional regulators previously associated to the defense reaction were *WRKY33*, transcriptional regulator involved in defense against *B*. *cinerea* and

Plasmopara viticola (Birkenbihl *et al*. 2012; Merz *et al*. 2015), and *Myb14*, which in grapevine regulates stilbene biosynthesis (Höll *et al*. 2013). This fast and strong induction of specific TFs leads to the activation of specific pathways, clearly related to plant defense. A number of genes encoding different classes of PR-proteins, such as chitinase, Bet v I allergen, and Beta 1-3 glucanase were upregulated, up to 40 fold. In this work, the transcription levels of *VvPR10.1* and *VvPR10.3*, and their regulator *WRKY33*, as indicated by previous studies for *VvPR10.1* (Dadakova *et al*. 2015; Merz *et al*. 2015), were analyzed in more detail. The transcription profiles measured by qPCR at five time points within the first 96hpi revealed that the transcript level of *VvWRKY33* was higher at 12 and 24 hpi (as compared to mock-treated samples) and dropped to the control level at later time points, 48 hpi and beyond, while the PR-proteins were always higher than control, except *VvPR10.1* at 48 hpi (Figure 6). Proteases including those involved in defense such as subtilisin-like protease, aspartic protease, and serine protease inhibitor were also more expressed in *Botryits*-inoculated than in mock-treated flowers (Supporting Information Data S8).

Secondary metabolism, mainly related to polyphenols, is upregulated in infected flowers

The RNA-Seq results underlined a reprogramming in secondary metabolism , especially at 24 hpi (Figure 4 and Supporting Information Data S8). Several genes related to terpenoid, benzoic acids, monolignol precursors, stilbenoid and flavonoid biosynthesis were strongly upregulated at 24 hpi. From the enrichment analysis, secondary metabolic process, protein modification process, and phenylpropanoid biosynthesis were among the enriched functional categories (Table 1 and Supporting Information Data S6). To confirm these RNA-Seq observations, targeted secondary metabolites, mainly polyphenols, were quantified by UHPLC-DAD-MS at five time points between 12 and 96 hpi. The analysis revealed that different classes of polyphenols were detected at higher concentrations in *Botrytis*-infected flowers as compared to mock-treated flowers (Supporting Information Data S9), suggesting a

defense-oriented metabolome reprogramming. Figure 7 shows a heat map of the concentrations of metabolites in correlation with gene expression profiles, taken from the RNA-Seq result. In the phenylpropanoid pathway, ten genes encoding PAL were upregulated, between 13 and 55 fold at 24 hpi (Supporting Information Data S8). Furthermore, genes encoding key enzymes in the pathway cinnamate 4-hydroxylase (C4H) and 4-coumarate-CoA ligase (4CL) had a fold change of about 12 and 4 times, respectively (Table 2). The concentrations of benzoic acids (*p*-hydroxybenzoic acid, vanillic acid, and gallic acid) and monolignol precursors (ferulic acid, caftaric acid, fertaric acid, and *trans*-coutaric acid) were generally higher in infected flowers (Figure 7A).

Regarding stilbenoids biosynthesis, a number of STS genes were highly upregulated at 24 hpi (Supporting Information Data S8). Of the 46 grapevine genes encoding for Stilbene Synthase (STS), more than 80% of them were expressed in the infected flowers with a relative induction between 15 and 90 fold. Two genes encoding VvMYB14, a TF regulating stilbene biosynthesis (Höll *et al*. 2013), were also upregulated at 24 hpi (Table 2), suggesting that this regulatory circuit is activated at 24 hpi. The expression profiles of *VvMYB14* and two STS genes, *VvSTS29* and *VvSTS41* were further monitored using qPCR (Figure 7B). Because of sequence similarity among STS genes (Vannozzi *et al*. 2012), the primers used for *VvSTS29* also detect the isoforms *VvSTS25* and *VvSTS27*, while the primers used for *VvSTS41* detect the isoform *VvSTS45* too (Höll *et al*. 2013). These results showed a strong coinduction between the *STS* genes and *VvMYB14* in grapevine flowers/fruitlets in response to *B*. *cinerea* infection. The expression patterns observed in the qPCR assay also fitted with the quantification of stilbenoids. The phytoalexin resveratrol and its monomeric-derivatives piceatannol and *trans*-piceid were detected at higher concentrations in the infected flowers/fruitlets than control (Figure 7A). The other monomers astringin and isorhapontin, both tetrahydroxystilbenes with antifungal activity (Hammerbacher *et al*. 2011), were also

induced. All of the quantified oligomeric resveratrols (dimers: *trans*-ε-viniferin, *cis*+*trans*-ω-viniferin, pallidol, ampelopsin D and quadrangularin A, and E-*cis*-miyabenol; trimers: Z-miyabenol C and α-viniferin; and the tetramer isohopeaphenol) were found highly concentrated in the infected flowers/fruitlets as compared to the control (Figure 7A). The quantities of the stress related *trans*-ε- and α-viniferins, which are also involved in grapevine–*Botrytis* interaction (Langcake 1981), ranged from 0.9 to 13.4 µg/g fresh weight (fw) and 2.8 to 151.8 µg/g fw, respectively, in the inoculated fruitlets as compared to basal levels in the controls. A similar increase in concentration was also observed in Z-miyabenol C and isohopeaphenol: 1.2 to 46.4 µg/g fw and 0.2 to 20.9µg/g fw, respectively (Supporting Information Data S9). Such an increase in the concentration of these stilbenoids suggests that they contribute to inhibiting the pathogen's advancement in colonizing the fruitlet.

In addition to *STS* genes, chalcone synthase (CHS), and dihydroflavonol-4-reductase (DFR), key flavonoid biosynthetic genes, were differentially expressed at 24 hpi (Table 2). The quantification of flavonoids revealed that flavanones, flavones, flavonols, and flavan-3-ols were detected at higher concentrations following *Botrytis* inoculation, most pronouncedly at 24, 72 and 96 hpi (Figure 7A). Flavonoids are also known to restrict fungal growth and in some cases also inhibit stilbene oxidases (Goetz *et al*. 1999; Guestsky *et al*. 2005; Puhl & Treutter 2008; Nagpala *et al*. 2016).

Infection triggers cell wall reinforcement

Reinforcing the cell wall to combat pathogen intrusion is a well-established mechanism in plants. A sign of cell wall apposition (CWA) at the site of penetration was observed by the autofluorescence of CWA regions (Figure 8A). The enrichment analyses also proposed that the L-phenylalanine catabolic process, and cell wall, were among the enriched functional classes (Supporting Information Data S6). This preliminary evidence was strengthened by modulation of genes encoding cell wall-modifying enzymes such as pectinesterases (PEs),

polygalacturonases (PGs), and pectate lyases (Supporting Information Data S8). Complementary to this, we observed that genes encoding germin-like protein 3 (GLP3) and proline-rich extensin-like protein (EXT), proteins involved in H_2O_2-mediated oxidative cross-linking to toughen cell walls during pathogen attack (Bradley *et al*. 1992; Godfrey *et al*. 2007; Kelloniemi *et al*. 2015), were highly upregulated both at 24 and 96 hpi (Table 2). Grapevine genes which encode enzymes involved in monolignol biosynthesis, cinnamyl alcohol dehydrogenase and *trans*-cinnamate 4-monooxygenase, were also highly upregulated (Table 2).

Cell wall reinforcement is one of the possible mechanisms by which the grapevine flower arrests the advancement of *Botrytis*. Ten genes encoding enzymes in the monolignol biosynthesis pathway (based on the VitisNet annotations of phenylpropanoid biosynthesis), were selected for further investigation with a qPCR assay. The quantities of L-phenylalanine and other seven intermediate metabolites in this pathway were also measured by HPLC-DAD-MS (Supporting Information Data S9). Transcripts of cinnamate 4-hydroxylase (*VvC4H*) and 4-coumarate-CoA ligase (*Vv4CL*), enzymes in the upstream of the pathway, were upregulated at the onset of *B*. *cinerea* infection, between 12 and 24 hpi, with *VvC4H* showing a peak at 12 hpi (Figure 8B). A similar trend was observed for cinnamoyl CoA reductase (*VvCCR*), the first enzyme specific to monolignol synthesis (Naoumkina *et al*. 2010). Caffeic acid o-methyltransferase (*VvCOMT*) and caffeoyl-CoA O-methyltransferase (*VvCCoAMT*) were upregulated at 24 hpi only; however, ferulate 5-hydroxylate (*VvF5H*) was upregulated throughout the post inoculation time points examined. Cinnamyl alcohol dehydrogenase (*VvCAD*) was significantly upregulated up to 48 hpi. In the cell wall, monolignols undergo oxidative polymerization, catalyzed by peroxidases/laccases (Naoumkina *et al*. 2010). A strong upregulation of a lignin-forming anionic peroxidase-like (*VvPER*) was observed, with the highest induction being within 24 hpi (Figure 8B). With

regard to laccase, 10 genes putatively encoding laccase, having the same KEGG enzyme code of *Arabidopsis* lignin laccase (Zhao *et al*. 2013), were also found extremely upregulated, up to 90 fold (Supporting Information Data S8). Pinoresinol/lariciresinol reductase (*VvPLR*) and secoisolariciresinol dehydrogenase (*VvSIRD*) genes, which catalyze subsequent metabolic steps to give rise to matairesinol, a lignan, as well as most of the DE genes which putatively encode dirigent-like proteins, a disease resistance-responsive family protein involved in lignan biosynthesis, were also upregulated in response to *B*. *cinerea*.

The quantification of metabolites also revealed that the concentrations of L-phenylalanine and cinnamate, which represent the two key entry substrates in the monolignol biosynthesis pathway, were significantly higher in *Botrytis*-inoculated flowers (Figure 8C). In contrast, the concentration of p-coumarate, caffeate, ferulate, and 5-hydroxyferulate were not different between *Botrytis*-inoculated flowers and control samples, probably due to their rapid conversion into the next metabolite of the pathway. Exceptions were the two intermediates, sinapaldehyde and coniferyl alcohol, metabolites found towards the end of the pathway, which were generally higher in the *Botryits*-inoculated flowers than in the control samples.

These results indicate that upon *B*. *cinerea* infection, cell wall fortification was among the defense mechanisms employed by the flowers/fruitlets to contain the pathogen in its quiescent state.

***B*. *cinerea* transcripts expressed *in planta* during grapevine flower infection**

The signal of *B*. *cinerea* transcripts detected in inoculated flowers was very low (Supporting Information Data S2 and Supporting Information Data S10). Therefore, it was not possible to perform a statistical comparison between the transcriptome of the infecting pathogen vs. the PDB-grown fungus, and an alternative approach was applied. Genes from *B*. *cinerea* were considered expressed if they were represented by an average of at least 10 reads in the three biological replicates of inoculated flower samples. 1325 genes met these conditions and will

be herein referred to as "*in planta* expressed genes". Of these 1325 genes, 751 and 59 were expressed only at 24 and 96 hpi, respectively; and 515 genes were expressed at both 24 and 96 hpi (Supporting Information Data S11).

Some of the *in planta* expressed genes exhibited high raw reads as compared to the others, but majority of them are annotated as predicted/ hypothetical proteins and ribosomal or housekeeping proteins. Other genes worth to mention because possibly involved in plant-fungus interaction are: *Bcin12g01020* and *Bcin14g00850*, encoding oxaloacetate and polygalacturonase, respectively; *Bcin03g00640* and *Bcin13g05810*, encoding putative alcohol oxidase and aldehyde dehydrogenase, respectively; *Bcin06g03370* encoding putative 4-dehydrocholesterol reductase precursor/ mitochondrial phosphate carrier 2; *Bcin05g04530* encoding putative ethylene receptor/ hsp90; and *Bcin02g07470* encoding putative byssal cuticle protein. In mussels, byssal cuticle facilitates its attachment to a substrate (Waite et al., 1989; Lee et al., 2011). The protein may also have a role in facilitating *Botrytis* attachment to the plant surface; its raw reads were higher at 24 than 96 hpi but almost no expression in PDB culture (Supporting Information Data S11).

The set of *in planta* expressed genes were functionally annotated using Blast2GO (Conesa *et al*. 2005) and Amselem *et al*. (2011) (Supporting Information Data S11). The joined biological meaning of the genes was visualized using the Combined Graph Function of Blast2GO based on their GO slim terms, and primary metabolic process, nitrogen compound metabolic process, ion binding, oxidoreductase activity, and cytoplasmic component were among the most represented GO terms (Supporting Information Data S12). The most important functional categories associated to the expressed genes are reported in Table 3. *In planta* expressed genes encompassed genes involved in pathogenesis, such as Carbohydrate-Active enZymes (CAZymes) devoted to plant cell wall degradation, in ROS production and

detoxification, in toxins biosynthesis, as well as in transcriptional regulation; all these genes were more abundant at 24 hpi. Besides, many ribosomal and histone genes were equally abundant at 24 and 96 hpi indicating the maintenance of a basal metabolism during quiescence.

B. cinerea genes required for pathogenesis are upregulated during flower infection

A group of 23 *in planta* expressed genes known to be related to *Botrytis* growth or pathogenesis were further characterized by qPCR. In addition, other two genes, glutathione S-transferase (*BcGST1*) and polygalacturonase 2 (*BcPG2*) were analyzed. qPCR expression profiles are shown in Figure 9, while gene names together with the expression level from the RNA-seq analysis are reported in Table 4.

All genes showed a sharp peak of expression at 24 hpi, except superoxide dismutase1 (*BcSOD1*), *BcGST1*, and the constitutively expressed *BcPG1*. Genes such as, oxaloacetate acetyl hydrolase (*BcOAH*), cutinase (*BcCUT-like1*), and pectate lyase (*BcPEL-like1*), appeared to be expressed exclusively during *Botrytis* attack, while other genes were also expressed in the absence of the host, but relatively much more during the host-pathogen interaction.

B. cinerea cutinases *BcCUTA* and *BcCUT*-like1are involved in the breaching of the cuticle layer by appressoria. This invasive step normally causes oxidative burst in the host (Schouten *et al*. 2002a) which is counteracted by the activation of scavenging mechanisms in the pathogen. The transcription levels of several *B. cinerea* genes taking part in the ROS-mediated fungus-plant interaction were quantified (Figure 9A). *BcSOD1*, which plays role in oxidative stress response during cuticle penetration (Rolke *et al*. 2004); H_2O_2 generators galactose oxidase (*BcGOX1*) and alcohol oxidase (*BcAOX*); ROS scavengers *BcGST*, peroxidase1 (*BcPRD1*), and glutathione peroxidase (*BcGPX3*) (Schumacher *et al*. 2014); and

BcLCC2, a gene involved in the oxidation of resveratrol and tannins (Schouten *et al*. 2002b), were all involved in the *Botrytis*-grapevine interaction.

A similar expression profile, albeit quantitavely different, was shown by cell wall-degrading enzymes (CWDEs) (Figure 9B). *PG*, pectate lyase (*BcPEL-like1*), and oxaloacetate acetyl hydrolase (*BcOAH*) are involved in pectin degradation. Galacturonate reductase (*BcGAR2*), galactonate dehydratase (*BcLGD1*), and 2-keto-3-deoxy-L- galactonate aldolase (*BcLGA1*), genes which play a role in the catabolic pathway of D-galacturonic acid (Zhang *et al*. 2011), a major component of pectin polysaccharides (Mohnen 2008; Caffall & Mohnen 2009), also had similar trends of expression. The strong and similar expression pattern in pectin and D-galacturonic acid degrading enzymes suggested that the degradation of the pectin backbone was initiated at 24 hpi. The involvement of other CWDEs, such as endo-beta-1,4-xylanase (*BcXYN11A*), which degrades hemicellulose and also induces necrosis (Noda *et al*. 2010), beta-glucosidase (*BcβGLUC*), which degrades both cellulose and hemicellulose (Gilbert 2010; Blanco-Ulate *et al*. 2014), and secreted aspartic proteinases (*AP*) was also highlighted from the qPCR assay (Figure 9B). The RNA-Seq data further suggested the involvement of pectin lyases (Bcin03g00280 and Bcin03g07360), enzyme acting preferentially on highly methyl esterified pectin, in the infection process (Supporting Information Data S11).

The strong upregulation of botcinic acid (*BcBOA*) and botrydial phytotoxins (*BcBOT*) genes, involved in phytotoxins synthesis, pointed towards their participation in the fungal infection program (Figure 9C).

Taken together, these results indicate the readiness of the fungus to colonize the flowers within 24 hpi. However, the transcript levels of all of the tested infection-related *B*. *cinerea* genes were much lower at 96 hpi, suggesting that the pathogenesis program initiated at 24 hpi is halted at a later time point. The transcriptional profile of *BcACTA* also suggested that the

activity of the fungus decreased towards the later hours of infection. From the post-inoculation inspection of the infected flowers, no visible disease progress was detected until ripening (Figure 1). This strengthens the hypothesis that the fungus reduced its biological activity and entered into a quiescent phase.

DISCUSSION

In grapevine, the epidemiology of the fungus, especially the infection process of the pathogen during flowering, is largely unknown. *B. cinerea* infection of grapevine inflorescence at blooming followed by a "latency period" was first reported by McClellan and Hewitt (1973). This observation was further confirmed by Keller *et al*. (2003) where inoculation at full bloom demonstrated causing high disease severity at harvest. Using the advantage of a GFP-labeled B05.10 strain, we could show for the first time that *B. cinerea* inoculated at flower cap-off stage remained in a quiescent state until berry full coloration (for about two and half months) and then it resumed active growth and invaded the berries when the microclimate was conducive (high humidity). This study provides a detailed description of the infection processes from infection initiation (24 hpi) to initial fungal quiescent (96 hpi) stages by means of transcriptomic and metabolic analyses and microscopic observations, laying the foundation for understanding the mechanism of the plant-fungus interaction during flowering which leads to pathogen quiescence.

Following the GFP fluorescence signal of the *Botrytis*, it was able to observe the penetration of the fungus into the flower cuticle within 24 hpi but no further appreciated growth at 96 hpi. Confocal microscopy and transcriptomic studies showed that the fungus, attempted to establish infection on grapevine flowers before becoming quiescent as observed from the germinated appressoria in the flower gynoecium (Figure 1B & G) and a prevalent modulation of defense related genes within 24 hpi. The main functional categories of the *in planta* expressed genes of the fungus were those related to pathogenesis (Table 3). Conidia

germination event of *B*. *cinerea* is accompanied by a rapid shift in gene expression, both for germtube outgrowth and host cell invasion (Leroch et al., 2013). Interestingly, much of these *in planta* expressed genes were also differentially regulated during successful infection of ripe grapevine berries (16, 24 and 48 hpi) (Kelloniemi *et al*. 2015), *Lactuca sativa* (12, 24, and 48 hpi) (De Cremer *et al*. 2013), and *Solanum lycopersicoides* (24 and 48 hpi) (Smith *et al*. 2014). This suggests that the *in planta* expressed genes were part of the pathogenesis mechanisms deployed in grapevine flowers that would help to establish infection.

One of the key processes in establishing infection by *B*. *cinerea* is the depolymerization of cell wall components (van Kan 2006; Williamson *et al*. 2007; Zhang *et al*. 2011). Generally, after breaching the cuticular layer of host tissues, *B*. *cinerea* often grows into the pectin-rich anticlinal wall of the underlying epidermal cell (van Kan 2006; Williamson *et al*. 2007), by the activation of pectinases. In our study, almost all of the assayed CWDEs were expressed at a higher level at 24 hpi (Figure 9). Besides increased levels of CWDEs, the upregulation of genes encoding the biosynthesis of phytotoxic secondary metabolites and secreted proteases, which assist the infection process (Dalmais *et al*. 2011; Rossi *et al*. 2011), further confirmed that the fungus put in place several strategies to invade the grapevine flowers. Nonetheless, there was no visible disease symptoms observed in the post-inoculation observations despite the presence of *B*. *cinerea* was confirmed by the plating out experiment (Figure 1H). The much lower number of *Botrytis* genes expressed *in planta* at 96 hpi as compared to 24 hpi (65% less), as well as the estimated ratio of *B*. *cinerea* to grapevine RNA (1:500, Supporting Information Data S2) compared to the much smaller ratio for genomic DNA (about 1:20, Figure 1I) in the same tissue, is also a confirmation that the fungus entered the quiescent phase.

Quiescence of a pathogen can happen before conidia germination, at initial hyphal development stage, before or after appressorium formation, after appressorium germination and/or at subcuticular hyphae stage (Prusky 1996). In unripe tomato, *Colletotrichum gloeosporioides* becomes quiescent as a swollen hyphae after appressorium germination (Alkan *et al*. 2015), whereas *Alternaria alternata* enters into quiescence after its hypha penetrates the cuticular layer of young apricot, persimmon, and mango fruits (Prusky 1996). For *B*. *cinerea*, cell wall penetrated hypha was proposed as a quiescent stage of infection in immature grape berries (Keller *et al*. 2003). Although the quiescence of ungerminated conidia cannot be completely ruled out in our case, the microscopic observation of conidia germination and appressoria formation (Figure 1G and Supporting Information Fig. S4), together with the results of the plating out experiment, which showed a non-significant effect of washing the inoculated berries (Figure 1H), indicate that the pathogen entered into a quiescent state after penetrating the cell wall. The burst of defense related reactions from the plant is also an indirect support for this claim.

In our study the attempted infection by *B*. *cinerea* instigated a multilayered defense response in the grapevine flower tissues. Following inoculation, more than 70 RLKs were differentially expressed within 24 hpi (Supporting Information Data S8). Several of these RLKs have been described to be involved in immune response to pathogens. The perception of cell wall fragments, such as oligogalacturonides (OGs) due to CWDE, induces basal resistance to the pathogen (Boller & Felix 2009). In *A*. *thaliana*, over-expressing the OG receptor *WAK1* enhanced resistance to *B*. *cinerea* (Brutus *et al*. 2010), but on the other hand increased susceptibility to *Sclerotinia sclerotiorum* and *B*. *cinerea* was observed in BAK1 mutant *Arabidopsis* (Kemmerling *et al*. 2007; Zhang *et al*. 2013). The RLK BAK1 constitutes a negative control element of microbial infection-induced cell death in plants (Kemmerling *et al*. 2007). These two *RLK*s exhibited increased expression levels in powdery mildew resistant

V. *pseudoreticulata* in response to *E*. *necator* (Weng *et al*. 2014) and in *B*. *cinerea* challenged lettuce (De Cremer *et al*. 2013). We also saw upregulation of genes coding for these membrane receptor proteins at 24 hpi, indicating that the plant recognized the pathogen and triggered immunity responses: quick and strong induction of PR-proteins and accumulation of stress related secondary metabolites, as well as cell wall lignification were deployed as major defense responses to halt the infection. The oxidative stress caused during the interaction seemed mainly managed by GSTs and ascorbate oxidases (Marrs 1996) as more than 20 genes coding for them were upregulated at 24 hpi. The pathogen responsive *PR10*, *PR5* (thaumatine-like protein), and chitinases also had a marked upregulation (between 5 and 40-fold upregulation within 24 hpi). *PR5* and chitinases are known for their inhibition of fungal growth including *B*. *cinerea* (Giannakis *et al*. 1998; Monteiro *et al*. 2003). From our qPCR result, a coordinated expression of *VvWRKY33*, *VvPR10.1* and *VvPR10.3* was demonstrated. *VvPR10.1* was recently associated to *P*. *viticola* resistance, in grapevine under the regulation of *VvWRKY33* (Merz *et al*. 2015). Even though the two pathogens are biologically different and may not necessarily activate similar response from their hosts, *VvPR10.1* and *VvPR10.3*, a PR belonging to the same group of *VvPR10.1* (Lebel *et al*. 2010), had the highest upregulation among the expressed PRs, making them strong candidates for the resistance of grapevine flower to *B*. *cinerea*. In *Arabidopsis WRKY33*, the functional homologue of *VvWRKY33* (Merz *et al*. 2015), plays a key role in the plant defense process, regulating redox homeostasis, SA signaling, ET-JA-mediated cross-communication, and phytoalexin biosynthesis conferring resistance to *B*. *cinerea* (Birkenbihl *et al*. 2012).

Upon *B*. *cinerea* infection, grapevine berries activate stilbenoid biosynthesis (Langcake 1981; Jeandet *et al*. 1995; Keller *et al*. 2003; Agudelo-Romero *et al*. 2015; Kelloniemi *et al*. 2015). Our results were in line with previous evidence. From the RNA-Seq results, it seemed that the genes coding for STS and laccase proteins were switched on following the infection,

since most of them were below the detection limit in the mock-inoculated flowers. The activation of the polyphenol biosynthetic pathway was further investigated by a more fine-grained expression profile of the transcription factor regulating stilbene biosynthesis (*VvMYB14*, Höll *et al*. 2013) together with *VvSTS29* and *VvSTS41*, and by measuring the concentration of several classes of polyphenols (phenylpropanoids, stilbenoids, and flavonoids). The phytoalexin resveratrol, which inhibits *B*. *cinerea* growth (Schouten *et al*. 2002b; Favaron *et al*. 2009) and its monomeric and oligomeric derivatives, some with documented antifungal activity (Hammerbacher *et al*. 2011), were all upregulated starting from 12 hpi. The concentrations of ε-viniferin and α-viniferin, dimer and trimer resveratrol respectively, were higher in *Botrytis*-infected flowers than control. These compounds represent the predominant stress metabolites in *Vitaceae-B*. *cinerea* interactions (Langcake 1981). We also observed a marked oligomerization of resveratrol to ampelopsin D and quadrangularin, E-cis-miyabenol, Z-miyabenol C, and isohopeaphenol upon infection, which agrees with the hypothesis that oligomerization of resveratrol leads to more toxic compounds (Pezet *et al*. 2003a). On the other hand, the glycosylated form of resveratrol, trans-piceid, were also shown to involve in *Colletotrichum higginsianum* resistance in *Arabidopsis* (Liu *et al*. 2011). A strong correlation was also observed between the concentration of stilbenic phytoalexins and resistance to *P*. *viticola* both in a *V*. *riparia* and *Merzling* × *Teroldego* cross population (Langcake 1981; Malacarne *et al*. 2011).

The potent stilbene oxidase inhibitors caftaric and *trans*-coutaric acids (both phenylpropanoids), catechin, and quercetin-3-O-glucuronide (both flavonoids) (Goetz *et al*. 1999) were also detected at higher concentrations in the *Botrytis*-infected flowers than in the control. These compounds possibly interfered with the fungal laccase activity by inactivating its oxidizing and insolubilizing effects on stilbenic phytoalexins and PR proteins (Goetz *et al*. 1999; Favaron *et al*. 2009). In addition, different classes of flavonoids including

proanthocyanidins (procyanidins B1, B2, B3 and B4) were also detected at a higher concentration in the infected flowers; these compounds can act as inhibitors of enzymes such as polygalacturonases. Higher concentration of proanthocyanidins in the epidermal layer of immature strawberry, at the periphery of *B. cinerea* penetration, was reported to restrict further growth of *B. cinerea* and keep the pathogen under quiescence (Jersch *et al*. 1989). Taken together, our results indicated a dramatic and rapid accumulation of the polyphenolic metabolites, in particular stilbenoids, at the site of infection suggesting this is a mechanism of defense to induce *B. cinerea* quiescence in grapevine flower.

Reinforcing cell walls is another strategy of plant resistance against pathogens. From our microscopic observations, cell wall apposition occurred at the appresorium penetration site (Figure 1F and Figure 8A). Gene expression and metabolite analysis also indicated that grapevine flowers, upon *B. cinerea* infection, activated the monolignol biosynthesis pathway within 24 hpi. A similar phenomenon occurs in wheat, where upregulation of monolignol genes within 24 hpi conferred resistance to *Blumeria graminis* f. sp. *Tritici*; and silencing a few key genes in the pathway (PAL, COMT, CCoAMT and CAD) compromised penetration resistance of the plant to the pathogen (Bhuiyan *et al*. 2009). The upregulation of *GLP3* and *EXT*, both at 24 and 96 hpi, and accumulation of H_2O_2 around the penetration site, as shown using the HyPer signal (Figure 5), suggests CWA was triggered as an early response to the infection. H_2O_2-mediated oxidative cross-linking and lignin synthesis to reinforce CWA and halt *B. cinerea* infection was recently shown in grapevine by Kelloniemi *et al*. (2015). In their study, the upregulation of lignin forming enzymes (GLP3 and EXT) together with the accumulation of H_2O_2, at the site of *Botrytis* penetration, were part of the defense mechanisms used by the véraison berry to arrest the pathogen. However, no such queues of responses were seen in the mature berry where the pathogen readily managed to colonize the berry tissue (Kelloniemi *et al*. 2015). In green tomatoes, usually resistant to *B. cinerea*, the

accumulation of H_2O_2 and lignin occurrs at the site of inoculation (Cantu *et al*. 2009), and in a tomato *sitiens* mutant, primed H_2O_2 accumulation and cell wall reinforcement were among the resistant factors against *B*. *cinerea* (Asselbergh *et al*. 2007). These all show that the CWA-mediated resistance was also active in the *B*. *cinerea* infected flowers.

The ability of grape berries in keeping the pathogen under quiescence is however broken at ripening (Supporting Information Fig. S6). This study was not designed to pinpoint the berry signals that trigger pathogen's transition from the prolonged quiescent to egression state. However, the changes in physical and chemical properties occurring at ripening, such as activation of phytohormone biosynthesis, cuticular changes, cell wall loosening, conversion of acids into sugars, and a steadily diminishing of antifungal compounds (both preformed and inducible secondary metabolites) are likely to favor pathogen egression (Prusky 1996; Prusky *et al*. 2013). Another factor that may modulate the transition from a quiescent to a necrotrophic state is the production of host signals, such as ethylene, which can trigger fungal pathogenicity factors (Prusky 1996). Alongside the decline in resistance uring ripening (Pezet *et al*. 2003b; Prusky & Lichter 2007), the sugars and organic acids exudates appearing on the berry surface during ripening (Padgett & Morrison 1990; Kretschmer *et al*. 2007) likely stimulate and promote *B*. *cinerea* outgrowth. In conclusion, the higher expression level of *B*. *cinerea* genes encoding for CWDE, phytotoxic secondary metabolites, and proteases within 24 hpi upon contact with the grapevine flower, indicated a readiness to establish a successful infection. However, there was no visible disease symptom for about 12 weeks, until the egression was apparent at the ripening stage. Flowers reacted readily to the infection as their defense mechanisms were very in-line upon recognizing the intruder. There was a marked accumulation of antimicrobial proteins (mainly PR-proteins), monolignol precursors, stilbenoids, and reactive oxygen species accompanied by cell wall reinforcement. The

conjugated actions of these induced defense responses seem to be responsible for forcing *B. cinerea* into quiescence until more favorable conditions occur in the berry.

AKNOWLEDGMENTS

The research was funded by the Autonomous Province of Trento (PAT-ADP 2013-2016). Z.M.H. is a recipient of FIRST scholarship from FEM. The authors would like to thank Domenico Masuero (FEM) for support with biochemical analysis, Dr. Alex Costa (University of Milan) for providing the HyPer construct, Daniele Brazzale (FEM) for his technical assistance, Dr. Ulrike Siegmund and Dr. Julia Schumacher (University of Muenster) for help with microscopy and for providing the GFP-labelled B05.10 strain of *B. cinerea*, Umberto Salvagnin (FEM) for taking pictures of the grapevine plants, and Dr. Giovanna Flaim for english revision of the manuscript.

REFERENCES

Agudelo-Romero P., Erban A., Rego C,. Carbonell-Bejerano P., Nascimento T., Sousa L., Martínez-Zapater J.M., ..., Fortes A.M. (2015) Transcriptome and metabolome reprogramming in *Vitis vinifera* cv. Trincadeira berries upon infection with *Botrytis cinerea*. *Journal of Experimental Botany* **66,** 1769–1785.

Alkan N., Friedlander G., Ment D., Prusky D. & Fluhr R. (2015) Simultaneous transcriptome analysis of *Colletotrichum gloeosporioides* and tomato fruit pathosystem reveals novel fungal pathogenicity and fruit defense strategies. *New Phytologist* **205,** 801–815.

Amselem J., Cuomo C.A., van Kan J.A., Viaud M., Benito E.P., Couloux A., …, Dickman M. (2011) Genomic analysis of the necrotrophic fungal pathogens *Sclerotinia sclerotiorum* and *Botrytis cinerea*. *PLoS Genetics* **7,** e1002230.

Asselbergh B., Curvers K., Franca S.C., Audenaert K., Vuylsteke, M.,Van Breusegem F. & Höfte M. (2007) Resistance to *Botrytis cinerea* in sitiens, an abscisic acid-deficient tomato mutant, involves timely production of hydrogen peroxide and cell wall modifications in the epidermis. *Plant Physiology* **144,** 1863-1877.

Bhuiyan N.H., Selvaraj G., Wei Y. & King J. (2009) Role of lignification in plant defense. *Plant Signaling & Behavior* **4,** 158–159.

Birkenbihl R.P., Diezel C. & Somssich I.E. (2012) Arabidopsis WRKY33 is a key transcriptional regulator of hormonal and metabolic responses toward *Botrytis cinerea* infection. *Plant Physiology* **159,** 266–285.

Blanco-Ulate B., Morales-Cruz A., Amrine K.C., Labavitch J.M., Powell A.L. & Cantu D. (2014) Genome-wide transcriptional profiling of *Botrytis cinerea* genes targeting plant cell walls during infections of different hosts. *Frontiers in Plant Science* **5,** 435.

Boller T. & Felix G. (2009) A renaissance of elicitors: perception of microbe- associated molecular patterns and danger signals by pattern-recognition receptors. *Annual Review of Plant Biology* **60,** 379–406.

Bradley D.J., Kjellbom P. & Lamb C.J. (1992) Elicitor- and wound- induced oxidative cross-linking of a proline-rich plant cell wall protein: A novel, rapid defense response. *Cell* **70,** 21-30.

Brutus A., Sicilia F., Macone A., Cervone F. & De Lorenzo G. (2010) A domain swap approach reveals a role of the plant wall–associated kinase 1 (WAK1) as a receptor of oligogalacturonides. *Proceedings of the National Academy of Sciences*, USA **107,** 9452–57.

Caffall K.H. & Mohnen D.B. (2009) The structure, function, and biosynthesis of plant cell wall pectic polysaccharides. *Carbohydrate Research* **344,** 1879–1900.

Cantu D., Blanco-Ulate B., Yang L., Labavitch J.M., Bennett A.B. & Powell A.L. (2009) Ripening-regulated susceptibility of tomato fruit to *Botrytis cinerea* requires NOR but not RIN or ethylene. *Plant Physiology* **150,** 1434-1449.

Choquer M., Fournier E., Kunz C., Levis C., Pradier J.M., Simon A. & Viaud M. (2007) *Botrytis cinerea* virulence factors: new insights into a necrotrophic and polyphagous pathogen. *FEMS Microbiology Letters* **277,** 1–10.

Coertze S. & Holz G. (2002) Epidemiology of *Botrytis cinerea* on grape: wound infection by dry, airborne conidia. *South African Journal for Enology and Viticulture* **23,** 72–77.

Conesa A., Götz S., García-Gómez J.M., Terol J., Talón M. & Robles M. (2005) Blast2GO: a universal tool for annotation, visualization and analysis in functional genomics research. *Bioinformatics* **21(18),** 3674–3676.

Costa A., Drago I., Behera S., Zottini M., Pizzo P., Schroeder J.I., Pozzan T. & Lo Schiavo F. (2010) H2O2 in plant peroxisomes: an in vivo analysis uncovers a Ca2+-dependent scavenging system. *The Plant Journal* **62,** 760-772.

Dadakova K., Havelkova M., Kurkova B., Tlolkova I., Kasparovsky T., Zdrahal Z. & Lochman J. (2015) Proteome and transcript analysis of *Vitis vinifera* cell cultures subjected to *Botrytis cinerea* infection. *Journal of Proteomics* **119,** 143–153.

Dalmais B., Schumacher J., Moraga J., Le Pecheur P., Tudzynski B., Collado I.G. & Viaud M. (2011) The *Botrytis cinerea* phytotoxin botcinic acid requires two polyketide synthases for production and has a redundant role in virulence with botrydial. *Molecular Plant Pathology* **12,** 564-579.

De Cremer K., Mathys J., Vos C., Froenicke L., Michelmore R.W., Cammue B.P. & De Coninck B. (2013) RNAseq-based transcriptome analysis of *Lactuca sativa* infected by the fungal necrotroph *Botrytis cinerea*. *Plant, Cell & Environment* **36,** 1992-2007.

Deytieux-Belleau C., Geny L., Roudet J., Mayet V., Donèche B. & Fermaud M. (2009) Grape berry skin features related to ontogenic resistance to Botrytis cinerea. *European Journal of Plant Pathology* **125,** 551-563.

Du Z., Zhou X., Ling Y., Zhang Z. & Su Z. (2010) agriGO: a GO analysis toolkit for the agricultural community. *Nucleic Acids Research* **38,** W64–W70.

Elmer P.A.G. & Michailides T.M. (2004) Epidemiology of Botrytis cinerea in orchard and vine crops. In: *Botrytis: Biology, Pathology and Control* (eds Y. Elad, B. Williamson, P. Tudzynski, & N. Delan), pp. 234-272. Kluwer Academic, Dordrecht, The Netherlands.

Eichorn K.W. & Lorenz D.H. (977) Phänologische entwicklungsstadien der rebe. *Nachrichtenblatt des Deutschen Pflanzenschutzdienstes* **29,** 119-120.

Espino J.J., Gutiérrez-Sánchez G., Brito N., Shah P., Orlando R. & González C. (2010) The *Botrytis cinerea* early secretome. *Proteomics* **10,** 3020–3034.

Favaron F., Lucchetta M., Odorizzi S., da Cunha A.T.P. & Sella L. (2009) The role of grape polyphenols on *trans*-resveratrol activity against *Botrytis cinerea* and of fungal laccase on the solubility of putative grape PR proteins. *Journal of Plant Pathology* **91,** 579-588.

Gao Q-M., Venugopal S., Navarre D. & Kachroo A. (2011) Low oleic acid- derived repression of jasmonic acid-inducible defense responses re- quires the WRKY50 and WRKY51 proteins. *Plant Physiology* **155,** 464–476.

Giannakis C., Bucheli C.S., Skene K.G.M., Robinson S.P. & Scott N.S. (1998) Chitinase and beta-1,3-glucanase in grapevine leaves: a possible defence against powdery mildew infection. *Australian Journal of Grape and Wine Research* **4,** 14–22.

Gilbert H.J. (2010) The biochemistry and structural biology of plant cell wall deconstruction. *Plant Physiology* **153,** 444–455.

Godfrey D., Able A.J. & Dry I.B. (2007) Induction of a grapevine germin-like protein (VvGLP3) gene is closely linked to the site of *Erysiphe necator* infection: A possible role in defense? *Molecular Plant-Microbe Interactions* **20,** 1112-1125.

Goetz G., Fkyerat A., Metais N., Kunz M., Tabacchi R., Pezet R. & Pont V. (1999) Resistance factors to grey mould in grape berries: Identification of some phenolics inhibitors of *Botrytis cinerea* stilbene oxidase. *Phytochemistry* **52,** 759-767.

Grimplet J., Van Hemert J., Carbonell-Bejerano P., Díaz-Riquelme J., Dickerson J., Fennell A., …, Martínez-Zapater J.M. (2012) Comparative analysis of grapevine whole-genome gene predictions, functional annotation, categorization and integration of the predicted gene sequences. *BMC Research Notes* **5,** 213.

Guetsky R., Kobiler I., Wang X., Perlman N., Gollop N., Avila-Quezada G., …, Prusky D. (2005) Metabolism of the flavonoid epicatechin by laccase of *Colletotrichum gloeosporioides* and its effect on pathogenicity on avocado fruits. *Phytopathology* **95 (11),** 1341− 1348.

Hammerbacher A., Ralph S.G., Bohlmann J., Fenning T.M., Gershenzon J. & Schmidt A. (2011) Biosynthesis of the major tetrahydroxystilbenes in spruce, astringin and isorhapontin, proceeds viaresveratrol and is enhanced by fungal infection. *Plant Physiology* **157(2),** 876–890.

Hellemans J., Mortier G., De Paepe A., Speleman F. & Vandesompele J. (2007) qBase relative quantification framework and software for management and automated analysis of real-time quantitative PCR data. *Genome Biology* **8,** R19.

Höll J., Vannozzi A., Czemmel S., D'Onofrio C., Walker A.R., Rausch T., …, Bogs J. (2013) The R2R3-MYB transcription factors MYB14 and MYB15 regulate stilbene biosynthesis in *Vitis vinifera*. *Plant Cell* **25,** 4135–4149.

Jaillon O., Aury J.M., Noel B., Policriti A., Clepet C., Casagrande A., …, French-Italian Public Consortium for Grapevine Genome Characterization (2007) The grapevine genome sequence suggests ancestral hexaploidization in major angiosperm phyla. *Nature* **449,** 463-467.

Jarvis W.R. (1962) The infection of strawberry and raspberry fruits by *Botrytis cinerea* Fr. *Annals of Applied Biology* **50,** 569–575.

Jarvis W.R. (1994) Latent infections in the pre- and post-harvest environment. *HortScience* **29,** 749–51.

Jeandet P., Bessis R., Sbaghi M. & Meunier P. (1995) Production of the phytoalexin resveratrol by grapes as a response to *Botrytis* attack under natural conditions. *Journal of Phytopathology* **143,**135-139.

Jersch S., Scherer C., Huth G. & Schlo□sser E. (1989) Proanthocyanidins as basis for quiescence of *Botrytis cinerea* in immature strawberry fruits *Z. Pflanzenkrankh Pflanzenschutz* **96,** 365−378.

Keller M., Viret O. & Cole M. (2003) *Botrytis cinerea* infection in grape flowers: defense reaction, latency and disease expression. *Phytopathology* **93,** 316–22.

Kelloniemi J., Trouvelot S., Heloir M.C., Simon A., Dalmais B., Frettinger P., …, Viaud M. (2015) Analysis of the molecular dialogue between graymold (*Botrytis cinerea*) and grapevine (*Vitis vinifera*) reveals a clear shift in defense mechanisms during berry ripening. *Molecular Plant-Microbe Interactions* **28,** 1167–1180.

Kemmerling B., Schwedt A., Rodriguez P., Mazzotta S., Frank M., Abu Qamar S., …, Nürnberger T. (2007) The BRI1- associated kinase 1, BAK1, has a Brassinoli-independent role in plant cell-death control. *Current Biology* **17,** 1116–1122.

Kretschmer M., Kassemeyer H.H. & Hahn M. (2007) Age-dependent grey mould susceptibility and tissue-specific defence gene activation of grapevine berry skins after infection by *Botrytis cinerea*. *Journal of Phytopathology* **155,**258-263.

Langcake P. (1981) Disease resistance of *Vitis* spp. and the production of the stress metabolites resveratrol, epsilon -viniferin, alpha - viniferin and pterostilbene. *Physiological Plant Pathology* **18,** 213-226.

Law C.W., Chen Y., Shi W. & Smyth G.K. (2014) Voom: Precision weights unlock linear model analysis tools for RNA-Seq read counts. *Genome Biology* **15(2),** R29.

Lebel S., Schellenbaum P.,Walter B. & Maillot P. (2010) Characterisation of the *Vitis vinifera* PR10 multigene family. *BMC Plant Biology* **10,** 184.

Lee P.P., messersmith P.B., Israelachvili J.N. & Waite J.H. (2011) Mussel inspired adhesives and coatings. *Annual Review of Materials Research* **41**, 99–132.

Leroch M., Kleber A., Silva E., Coenen T., Koppenhöfer D., Shmaryahu A., Valenzuela P.D.T. & Hahn M. (2013) Transcriptome profiling of Botrytis cinerea conidial germination reveals upregulation of infection-related genes during the prepenetration stage. *Eukaryotic Cell* **12**, 614–26.

Leroch M., Mernke D., Koppenhoefer D., Schneider P., Mosbach A., Doehlemann G. & Hahn M. (2011) Living colors in the gray mold pathogen Botrytis cinerea: codon-optimized genes encoding green fluorescent protein and mCherry, which exhibit bright fluorescence. *Applied and Environmental Microbiology* **77**, 2887–97.

Liao Y., Smyth G.K. & Shi W. (2013) The Subread aligner: fast, accurate and scalable read mapping by seed-and-vote. *Nucleic Acids Research* **41,** e108.

Liao Y., Smyth G.K. & Shi W. (2014) featureCounts: an efficient general-purpose program for assigning sequence reads to genomic features. *Bioinformatics* **30(7),** 923-930.

Lijavetzky D., Carbonell-Bejerano P., Grimplet J., Bravo G., Flores P., Fenoll J., …, Martínez-Zapater J.M. (2012) Berry flesh and skin ripening features in *Vitis vinifera* as assessed by transcriptional profiling. *PLoS ONE* **7,** e39547.

Liu Z.Y., Zhuang C.X. & Sheng S.J. (2011) Overexpression of a resveratrol synthase gene (PcRs) from *Polygonum cuspidatum* in transgenic *Arabidopsis* causes the accumulation of trans-piceid with antifungal activity. *Plant Cell Reports* **30,** 2027–2036.

Malacarne G., Vrhovsek U., Zulini L., Cestaro A., Stefanini M., Mattivi F., …, Moser, C. (2011) Resistance to *Plasmopara viticola* in a grapevine segregating population is associated with stilbenoid accumulation and with specific host transcriptional responses. *BMC Plant Biology* **11,** 114.

Marrs K.A. (1996) The functions and regulation of glutathione *S*-transferases in plants. *Annual Review of Plant Physiology and Plant Molecular Biology* **47,** 127–158.

Martin M. (2011) Cutadapt removes adapter sequences from high-throughput sequencing reads. *EMBnetjournal* **17,** 10–12.

McNicol R.J. & Williamson B. (1989) Systemic infection of blackcurrant flowers by *Botrytis cinerea* and its possible involvement in premature abscission of fruits. *Annals of Applied Biology* **114,** 243–254.

McClellan W.D. & Hewitt W.B. (1973) Early *Botrytis* rot of grapes: Time of infection and latency of *Botrytis cinerea* Pers. in L. *Phytopathology* **63,** 1151-1157.

Merz P.R., Moser T., Höll J., Kortekamp A., Buchholza G., Zyprian E. & Bogs J. (2015) The transcription factor VvWRKY33 is involved in the regulation of grapevine (*Vitis vinifera*) defense against the oomycete pathogen *Plasmopara viticola*. *Physiologia Plantarum* **153,** 365–380.

Mlikota-Gabler F., Smilanick J.L., Mansour M., Ramming D.W. & Mackey B.E. (2003) Correlation of morphological, anatomical, and chemical features of grape berries with resistance to *Botrytis cinerea*. *Phytopathology* **93,** 1263–1273.

Mohnen D. (2008) Pectin structure and biosynthesis. *Current Opinion in Plant Biology* **11,** 226–277.

Monteiro S., Barakat M., Picarra-Pereira M.A., Teixeira A.R. & Ferreira R.B. (2003) Osmotin and thaumatin from grape: a putative general defense mechanism against pathogenic fungi. *Phytopathology* **93,** 1505-1512.

Moretto M., Sonego P., Dierckxsens N., Brilli M., Bianco L., Ledezma-Tejeida D., ..., Engelen K. (2016) COLOMBOS v3.0: leveraging gene expression compendia for cross-species analyses. *Nucleic Acids Research* **44(D1),** D620-3.

Mullins M.G. & Rajaskekaren K. (1981) Fruiting cuttings: Revised method for producing test plants of grapevine cultivars. *American Journal of Enology and Viticulture* **32,** 35-40.

Nagpala E.G., Guidarelli M., Gasperotti M., Masuero D., Bertolini P., Vrhovsek U. & Baraldi E. (2016) Polyphenols Variation in Fruits of the Susceptible Strawberry Cultivar Alba during Ripening and upon Fungal Pathogen Interaction and Possible Involvement in Unripe Fruit Tolerance. *Journal of Agricultural and Food Chemistry* **64(9),** 1869-78.

Nair N.G., Guilbaud-Oulton S., Barchia I. & Emmett R. (1995) Significance of carry over inoculum, flower infection and latency on the incidence of *Botrytis cinerea* in berries of grapevines at harvest *Vitis vinifera* in New South Wales. *Australian Journal of Experimental Agriculture* **35,** 1177-1180.

Naoumkina M.A., Zhao Q., Gallego-Giraldo L., Dai X., Zhao P.X. & Dixon R.A. (2010) Genome-wide analysis of phenylpropanoid defence pathways. *Molecular Plant Pathology* **11,** 829–846.

Noda J., Brito N. & Gonzalez C. (2010) The *Botrytis cinerea* xylanase Xyn11A contributes to virulence with its necrotizing activity, not with its catalytic activity. BMC Plant Biolology **10,** 38.

Padgett M. & Morrison J.C. (1990) Changes in the grape berry exudates during fruit development and their effect on the mycelial growth of *Botrytis cinerea*. *Journal of the American Society for Horticultural Science* **115,** 269–273.

Pezet R., Perret C., Jean-Denis J.B., Tabacchi R., Gindro K. & Viret O. (2003a) δ-Viniferin, a resveratrol dehydrodimer: one of the major stilbenes synthesized by stressed grapevine leaves. *Journal of Agricultural and Food Chemistry* **51,** 5488–5492.

Pezet R., Viret O., Perret C. & Tabacchi R. (2003b) Latency of *Botrytis cinerea* Pers.: Fr. and biochemical studies during growth and ripening of two grape berry cultivars, respectively susceptible and resistant to grey mould. *Journal of Phytopathology* **151,** 208-214.

Prusky D. (1996) Pathogen quiescence in postharvest diseases. *Annual Review of Phytopathology* **34,** 413- 434.

Prusky D., Alkan N., Mengiste T. & Fluhr R. (2013) Quiescent and necrotrophic lifestyle choice during postharvest disease development. *Annual Review of Phytopathology* **51,** 155–176.

Prusky D. & Lichter A. (2007) Activation of quiescent infections by postharvest pathogens during transition from the biotrophic to the necrotrophic stage. *FEMS Microbiology Letters* **268,** 1–8.

Puhl I. & Treutter D. (2008) Ontogenetic variation of catechin biosynthesis as basis for infection and quiescence of Botrytis cinerea in developing strawberry fruits. *Journal of Plant Diseases and Protection* **115,** 247−251.

Rieu I. & Powers S.J. (2009) Real-time quantitative RT-PCR: design, calculations, and statistics. *Plant Cell* **2,** 1031–1033.

Rolke Y., Liu S., Quidde T., Williamson B., Schouten S., Weltring K.M., …, Tudzynski P. (2004) Functional analysis of H2O2-generating systems in *Botrytis cinerea*: the major Cu-Zn-superoxide dismutase (BCSOD1) contributes to virulence on French bean, whereas a glucose oxidase (BCGOD1) is dispensable. *Molecular Plant Pathology* **5,** 17–27.

Rossi F.R., Garriz A., Marina M., Romero F.M., Gonzalez M.E., Collad I.G. & Pieckenstain F.L. (2011) The sesquiterpene botrydial produced by *Botrytis cinerea* induces the hypersensitive response on plant tissues and its action is modulated by salicylic acid and jasmonic acid signaling. *Molecular Plant-Microbe Interactions* **24,** 888–896.

Ruijter J.M., Ramakers C., Hoogaars W.M., Karlen Y., Bakker O., van den Hoff M. J. and Moorman A.F. (2009) Amplification efficiency: Linking baseline and bias in the analysis of quantitative PCR data. *Nucleic Acids Research* **37,** e45.

Schouten A., Tenberge K.B., Vermeer J., Stewart J., Wagemakers C.A.M., Williamson B. & van Kan J.A.L. (2002a) Functional analysis of an extracellular catalase of *Botrytis cinerea*. *Molecular Plant Pathology* **3,** 227–238.

Schouten A., Wagemakers L., Stefanato F.L., van der Kaaij R.M. & van Kan J.A.L. (2002b) Resveratrol acts as a natural profungicide and induces self-intoxication by a specific laccase. *Molecular Microbiology* **43,** 883-894.

Schumacher J. (2012) Tools for Botrytis cinerea : New expression vectors make the gray mold fungus more accessible to cell biology approaches. *Fungal Genetics and Biology* **49**, 483–497.

Schumacher J., Simon A., Cohrs K.C., Viaud M. & Tudzynski P. (2014) The transcription factor BcLTF1 regulates virulence and light responses in the necrotrophic plant pathogen *Botrytis cinerea*. *PLoS Genetics* **10,** e1004040.

Shaw M.W., Emmanuel C.J., Emilda D., Terhem R.B., Shafia A., Tsamaidi D., …, van Kan J.A.L. (2016) Analysis of cryptic, systemic *Botrytis* infections in symptomless hosts. *Frontiers in Plant Science* **7,** 625.

Smith J.E., Mengesha B., Tang H., Mengiste T. & Bluhm B.H. (2014) Resistance to *Botrytis cinerea* in *Solanum lycopersicoides* involves widespread transcriptional reprogramming. *BMC Genomics* **15,** 334.

Smyth G.K. (2004) Linear models and empirical bayes methods for assessing differential expression in microarray experiments. *Statistical Applications in Genetics and Molecular Biology* **3,** 3.

Thimm O., Bläsing O., Gibon Y., Nagel A., Meyer S., Krüger P., …, Stitt M. (2004) MAPMAN: a user-driven tool to display genomics data sets onto diagrams of metabolic pathways and other biological processes. *The Plant Journal* **37,** 914–939.

Vandesompele J., De Preter K., Pattyn F., Poppe B., van Roy N., De Paepe A. & Speleman F. (2002) Accurate normalization of real-time quantitative RT-PCR data by geometric averaging of multiple internal control genes. *Genome Biology* **3(7),** RESEARCH0034.

van Kan J.A.L. (2006) Licensed to kill: the lifestyle of a necrotrophic plant pathogen. *Trends Plant Science* **11**: 247-253

van Kan J.A.L., Shaw M.W. & Grant-Downton R.T. (2014) *Botrytis* species: relentless necrotrophic thugs or endophytes gone rogue? Molecular Plant Pathology **15(9),** 957–961.

van Kan J.A.L., Stassen J.H.M., Mosbach A., van Der Lee T.A.J., Faino L., Farmer A.D., …, Scalliet G. (2016) A gapless genome sequence of the fungus *Botrytis cinerea*. *Molecular Plant Pathology* DOI**,** 10.1111/mpp.12384.

Vannozzi A., Dry I.B., Fasoli M., Zenoni S. & Lucchin M. (2012) Genome-wide analysis of the grapevine stilbene synthase multigenic family: genomic organization and expression profiles upon biotic and abiotic stresses. *BMC Plant Biology* **12,** 130.

Velasco R., Zharkikh A., Troggio M., Cartwright D.A., Cestaro A., Pruss D., …, Viola R. (2007) A high quality draft consensus sequence of the genome of a heterozygous grapevine variety. *PLoS ONE* **2,** e1326.

Volodarsky D., Leviatan N., Otcheretianski A. & Fluhr R. (2009) HORMONOMETER: a tool for discerning transcript sig- natures of hormone action in the Arabidopsis transcriptome. *Plant Physiology* **150,** 1796–1805.

Vrhovsek U., Masuero D., Gasperotti M., Franceschi P., Caputi L.,Viola R. & Mattivi F. (2012) A versatile targeted metabolomics method for the rapid quantification of multiple classes of phenolics in fruits and beverages. *Journal of Agricultural and Food* C*hemistr*y **60**(36)**,** 8831−8840.

Waite J.H., Hansen D.C., & Little K.T. (1989) The glue protein of ribbed mussels (*Geukensia demissa*): a natural adhesive with some features of collagen. *Journal of Comparative Physiology B* **159**:517–525.

Weng K., Li Z.Q., Liu R.Q., Wang L., Wang Y.J. & Xu Y. (2014) Transcriptome of *Erysiphe necator* infected *Vitis pseudoreticulata* leaves provides insight into grapevine resistance to powdery mildew. *Horticulture Research* **1,** 14049.

Wiermer M., Feys B.J. & Parker J.E. (2005) Plant immunity: the EDS1 regulatory node. *Current Opinion in Plant Biology* **8,** 383–389.

Williamson B., McNicol R.J. & Dolan A. (1987) The effect of inoculating flowers and developing fruits with *Botrytis cinerea* on post-harvest grey mould of red raspberry. *Annals of Applied Biology* **111,** 285-294.

Williamson B., Tudzynski B., Tudzynski P. & van Kan J.A.L. (2007) *Botrytis cinerea*: the cause of grey mould disease. *Molecular Plant Pathology* **8,** 561–580.

Zhang L., Thiewes H. & van Kan J.A.L. (2011) The D-galacturonic acid catabolic pathway in *Botrytis cinerea*. *Fungal Genetics and Biology* **48,** 990–997.

Zhang W., Fraiture M., Kolb D., Löffelhardt B., Desaki Y., Boutrot F.F., …, Brunner, F. (2013) *Arabidopsis* RECEPTOR- LIKE PROTEIN30 and receptor-like kinase SUPPRESSOR OF BIR1-1/ EVERSHED mediate innate immunity to necrotrophic fungi. *Plant Cell* **25,** 4227–4241.

Zhao Q., Nakashima J., Chen F., Yin Y., Fu C., Yun J., …, Dixon R.A. (2013) Laccase is necessary and nonredundant with peroxidase for lignin polymerization during vascular development in *Arabidopsis*. *Plant Cell* **25,** 3976–3987.

Tables

Table 1. Enriched Grapevine Molecular Networks according to VitisNet annotation

VVID	Network Name	Description	Number in input list	Number in reference list	*p*-value
Upregulated genes (24 hpi)					
10530	Aminosugars metabolism	carbohydrate metabolism	9	76	1.15E-03
10910	Nitrogen metabolism	energy metabolism	8	83	2.04E-03
10350	Tyrosine metabolism	amino acid metabolism	10	130	3.23E-03
10460	Cyanoamino acid metabolism	other amino acids metabolism	4	31	9.99E-03
10480	Glutathione metabolism	other amino acids metabolism	16	127	4.14E-07
10770	Pantothenate and CoA biosynthesis	cofactors and vitamin metabolism	5	39	4.16E-03
10940	Phenylpropanoid biosynthesis	biosynthesis of secondary metabolites	40	187	2.00E-12
11000	Single reactions	other	11	154	3.65E-03
34020	Calcium signaling pathway	signal transduction	9	128	9.05E-03
30008	Ethylene signaling	hormone signaling	15	232	2.00E-03
34626	Plant-pathogen interaction	plant specific signaling	25	311	1.75E-06
60003	AP2/EREBP	transcription factor	10	131	3.41E-03
60066	WRKY	transcription factor	19	62	1.93E-11
60069	ZIM	transcription factor	4	13	3.36E-04
Downregulated genes (24 hpi)					
10500	Starch and sucrose metabolism	carbohydrate metabolism	12	324	2.71E-04
44110	Cell cycle	cell growth and death	21	316	3.85E-11
44810	Regulation of actin cytoskeleton	cell motility	27	340	5.85E-16
60076	Other GTF		2	6	1.79E-03
Upregulated genes (96 hpi)					
10640	Propanoate metabolism	carbohydrate metabolism	4	63	6.66E-04
50121	Porters cat 1 to 6	transporter catalogue	6	160	5.20E-04
Downregulated genes (96 hpi)					
40006	cell wall	cell growth and death	12	445	1.31E-07

Table 2. Selected differentially expressed grapevine genes from *B. cinerea* inoculation at 24 and 96 hpi

Id	Fold change (log2) 24 hpi	96 hpi	Functional annotation
Recognition and signaling			
VIT_15s0046g02220	2.67		ACC synthase
VIT_07s0031g01070	2.21		Ascorbate oxidase
VIT_14s0030g02150	2.04	2.33	Calmodulin
VIT_11s0016g03080	1.42		Clavata1 receptor kinase (CLV1)
VIT_12s0035g00610	6.01		CYP82M1v3
VIT_18s0001g00030	1.01	2.79	CYP87A2
VIT_17s0000g07400	1.01		Disease resistance protein (EDS1)
VIT_17s0000g07420	1.38		Enhanced disease susceptibility 1 (EDS1)
VIT_02s0234g00130	1.60		Ethylene responsive element binding factor 1
VIT_15s0048g01350	2.22		Gibberellin receptor GID1L3
VIT_08s0040g00920	2.94	1.71	Glutathione S-transferase 25 GSTU7
VIT_11s0016g00710	0.83		Jasmonate ZIM-domain protein 1
VIT_01s0011g03650	2.21		Map kinase substrate 1 MKS1
VIT_00s0250g00090	4.42	2.72	Oxidoreductase, 2OG-Fe(II) oxygenase
VIT_03s0063g02440		-1.71	Proline extensin-like receptor kinase 1 (PERK1)
VIT_13s0064g01790	-1.62		R protein MLA10
VIT_00s0748g00020	4.14		Receptor kinase RK20-1
VIT_17s0000g04400	1.38		Wall-associated kinase 1 (WAK1)
Trascription factors			
VIT_07s0005g03220	3.53		ERF098
VIT_11s0016g02070	3.09	1.43	Basic helix-loop-helix (bHLH) family
VIT_07s0005g03340	1.87		Myb domain protein 14
VIT_19s0027g00860	3.64		NAC domain-containing protein 42
VIT_08s0058g00690	1.65		WRKY DNA-binding protein 33
VIT_14s0068g01770	3.29		WRKY DNA-binding protein 75
Cell wall			
VIT_14s0128g00970	2.75	1.40	Germin-like protein 3
VIT_05s0077g01280	-1.72	-2.40	Glycosyl hydrolase family 3 beta xylosidase (BXL1)
VIT_06s0009g02560	3.21		Pectinesterase family
VIT_08s0007g08330	-4.80		Polygalacturonase PG1
VIT_09s0054g01080	3.10		Polygalacturonase QRT3
VIT_06s0004g01990	4.87	3.15	Proline-rich extensin-like family protein
VIT_03s0017g01990	1.79		UDP-glucose glucosyltransferase

Id	Fold change (log2) 24 hpi	96 hpi	Functional annotation
Response to stress and secondary metabolism			
VIT_18s0001g04280	5.07		(-)-germacrene D synthase
VIT_11s0052g01110	1.96		4-coumarate-CoA ligase 1
VIT_04s0008g07250	2.04		Aspartyl protease
VIT_05s0077g01540	5.43		Bet v I allergen
VIT_16s0098g00850	0.68		Caffeic acid O-methyltransferase
VIT_16s0100g00860	4.99		Chalcone synthase
VIT_11s0149g00280	2.13		Chitinase A
VIT_03s0180g00250	4.41		Cinnamyl alcohol dehydrogenase
VIT_16s0039g02350	1.07		Dihydroflavonol 4-reductase
VIT_18s0122g01150	6.57	2.61	Diphenol oxidase
VIT_06s0004g01020	5.62	2.10	Dirigent protein
VIT_07s0031g01380	2.04	0.96	ferulate 5-hydroxylase
VIT_05s0020g05000	1.70		Inhibitor of trypsin and hageman factor (CMTI-V)
VIT_18s0001g00850	6.48	2.84	Laccase
VIT_16s0098g00460	3.29		Lipase class 3
VIT_14s0083g00850		-1.67	Lipase GDSL 7
VIT_13s0067g00050	3.32		Myrcene synthase
VIT_15s0048g02430	1.65		Naringenin,2-oxoglutarate 3-dioxygenase
VIT_05s0077g01530	4.94	1.56	Pathogenesis protein 10
VIT_05s0077g01550	4.62		Pathogenesis protein 10.3
VIT_03s0088g00750	1.45		Pathogenesis related protein 1 precursor
VIT_01s0010g02020	7.12	2.09	Peroxidase
VIT_16s0039g01280	5.40		Phenylalanin ammonia-lyase
VIT_00s2849g00010	5.83		Phenylalanine ammonia-lyase
VIT_02s0025g02920	1.67		Quercetin 3-O-methyltransferase 1
VIT_08s0058g00790	1.51		Secoisolariciresinol dehydrogenase
VIT_16s0100g01010	4.64		Stilbene synthase (VvSTS29)
VIT_16s0100g01130	4.34		Stilbene synthase (VvSTS41)
VIT_16s0100g01160	4.39		Stilbene synthase (VvSTS45)
VIT_16s0100g00990	4.60		Stilbene synthase 2 (VvSTS27)
VIT_16s0100g00950	4.63		Stilbene synthase 3 (VvSTS25)
VIT_02s0025g04230	2.21		Thaumatin
VIT_11s0065g00350	3.54		Trans-cinnamate 4-monooxygenase

Table 3. Specific functions of *in planta* detected *B. cinerea* transcripts

Functions of of *Botrytis cinerea* genes	No.of genes involved	
	24hpi	96hpi
Proteins identified as early secretome, within 16 h of germination (Espino *et al*. 2010)	39	9
Carbohydrate-Active Enzymes (CAZymes) (Amselem *et al*. 2011; Blanco-Ulate *et al*. 2014)	203	64
CAZymes acting on fungal cell wall	36	16
CAZymes acting on plant cell wall	56	11
CAZymes acting on cellulose	5	2
CAZymes acting on hemicellulose	20	3
CAZymes acting on hemicellulose and pectin side chains	9	0
CAZymes acting on pectin	23	1
Proteins generating Reactive Oxygen Species (ROS) (Schumacher *et al*. 2014)	10	2
Proteins involved in the detoxification of ROS (Schumacher *et al*. 2014)	23	8
Protease (Amselem *et al*. 2011)	38	8
secondary metabolism key enzymes (Amselem *et al*. 2011)	3	0
60S & 40S ribosomal protein (Amselem *et al*. 2011)	78	78
Appressorium-associated genes (orthologs in *Magnaporthe oryzae*) (Amselem *et al*. 2011)	7	2
Transporters	64	22
Transcription factors	29	13
Histone	8	7
Actin	11	6

Table 4. RNA-seq reads of *B*. *cinerea* transcripts checked by qPCR assay

			Average no. of raw reads from RNA-seq analysis		
			In planta expressed		PDB culture
Abbreviation	Transcript description	Gene ID	24hpi	96hpi	
BcSOD1	Superoxide dismutase1	Bcin03g03390	76	26	9411[a]
BcGOX1	Galactose oxidase	Bcin13g05710	21		609
BcAOX	Alcohol oxidase	Bcin07g03040	24		490
BcGST1	Glutathione S-transferase	Bcin10g00740			2655[a]
BcPRD1	Dyp-type peroxidase	Bcin13g05720	19		312
BcGPX3	Glutathione peroxidase	Bcin03g01480	23		2871[a]
BcLCC2	Laccase2	Bcin14g02510	15		32[b]
BcCUTA	Cutinase	Bcin15g03080	15		54[b]
BcCUT-like1	Cutinase	Bcin01g09430	68	11	9[b]
BcOAH	Oxaloacetate acetylhydrolase	Bcin12g01020	386		38[b]
BcPG1	Polygalacturonase1	Bcin14g00850	209	175	147821[a]
BcPG2	Polygalacturonase2	Bcin14g00610			362
BcPG4	Polygalacturonase4	Bcin03g01680	44		47[b]
BcPG6	Polygalacturonase6	Bcin02g05860	75		62
BcPEL-like1	Pectate lyase	Bcin03g05820	87	24	40[b]
BcGAR2	D-galacturonic acid reductase2	Bcin03g01500	37		104
BcLGD1	D-galactonate dehydrogenase	Bcin01g09450	61	10	804
BcLGA1	2-keto-3-deoxy-L-galactonate aldolase	Bcin03g01490	70	13	66
BcXYN11A	Endo-beta-1,4-xylanase	Bcin03g00480	18		129
BcβGLUC	Beta-glucosidase 1 precursor	Bcin10g05590	32		75
BcAP8	Aspartic proteinase8	Bcin12g02040	30	12	1064[a]
BcAP9	Aspartic proteinase9	Bcin12g00180	16		569
BcBOT1	Botrydial biosynthesis1	Bcin12g06380	58		86
BcBOT2	Botrydial biosynthesis2	Bcin12g06390	41		55
BcBOA6	Botcinic acid6	Bcin01g00060	13		1048[a]

(a) transcripts whose average raw reads is in the top 25 %, most expressed, while (b) are those transcripts whose average reads is in the bottom 25 %, least expressed, in PDB culture.

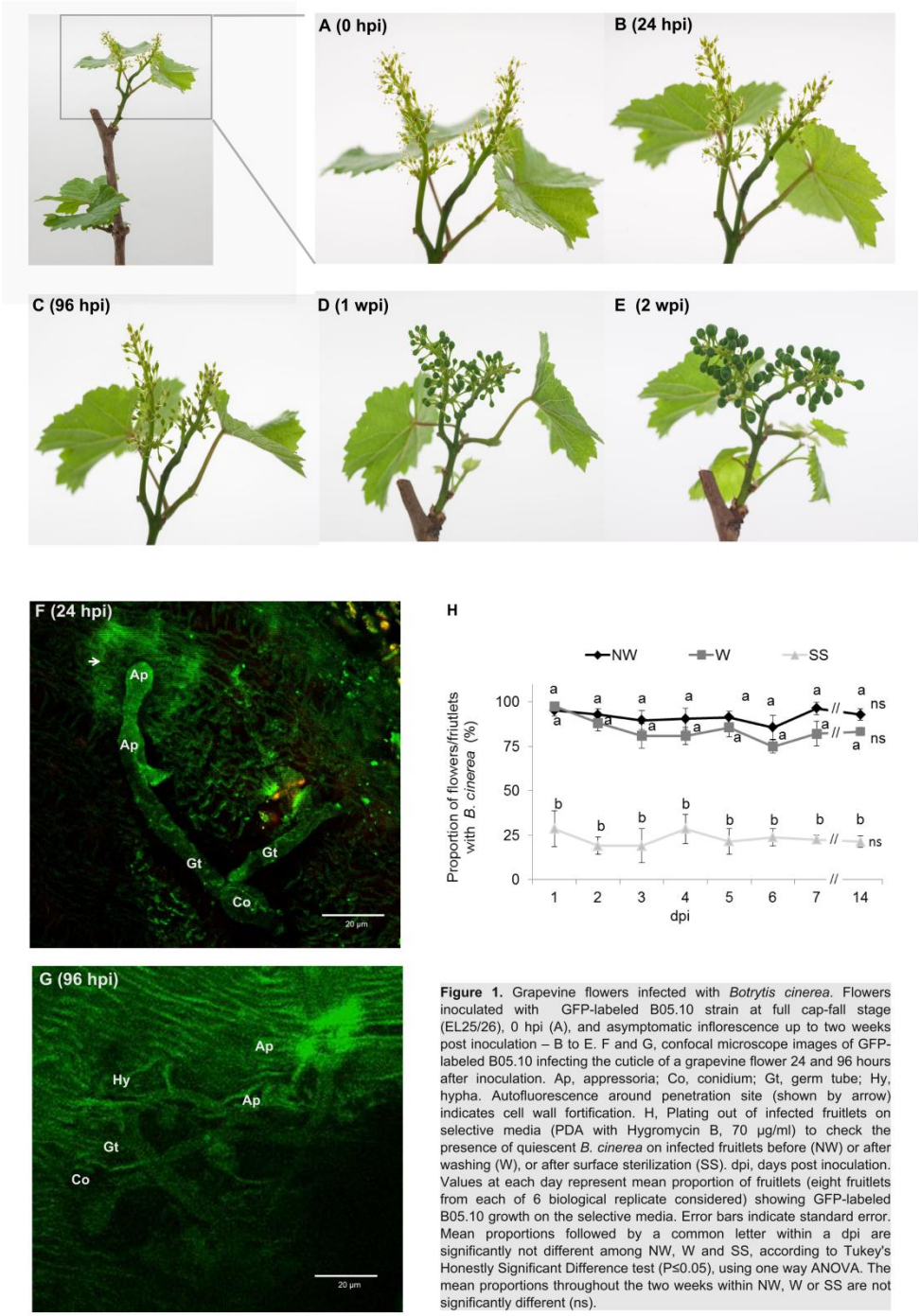

Figure 1. Grapevine flowers infected with *Botrytis cinerea*. Flowers inoculated with GFP-labeled B05.10 strain at full cap-fall stage (EL25/26), 0 hpi (A), and asymptomatic inflorescence up to two weeks post inoculation – B to E. F and G, confocal microscope images of GFP-labeled B05.10 infecting the cuticle of a grapevine flower 24 and 96 hours after inoculation. Ap, appressoria; Co, conidium; Gt, germ tube; Hy, hypha. Autofluorescence around penetration site (shown by arrow) indicates cell wall fortification. H, Plating out of infected fruitlets on selective media (PDA with Hygromycin B, 70 µg/ml) to check the presence of quiescent *B. cinerea* on infected fruitlets before (NW) or after washing (W), or after surface sterilization (SS). dpi, days post inoculation. Values at each day represent mean proportion of fruitlets (eight fruitlets from each of 6 biological replicate considered) showing GFP-labeled B05.10 growth on the selective media. Error bars indicate standard error. Mean proportions followed by a common letter within a dpi are significantly not different among NW, W and SS, according to Tukey's Honestly Significant Difference test (P≤0.05), using one way ANOVA. The mean proportions throughout the two weeks within NW, W or SS are not significantly different (ns).

Figure 1. Grapevine flowers infected with *Botrytis cinerea*. Flowers inoculated with GFP-labeled B05.10 strain at full cap-fall stage (EL25/26), 0 hpi (A), and asymptomatic inflorescence up to two weeks post inoculation – B to E. F and G, confocal microscope images of GFP-labeled B05.10 infecting the cuticle of a grapevine flower 24 and 96 hours after inoculation. Ap, appressoria; Co, conidium; Gt, germ tube; Hy, hypha.

Autofluorescence around penetration site (shown by arrow) indicates cell wall fortification. H, Plating out of infected fruitlets on selective media (PDA with Hygromycin B, 70 μg/ml) to check the presence of quiescent *B. cinerea* on infected fruitlets before (NW) or after washing (W), or after surface sterilization (SS). dpi, days post inoculation. Values at each day represent mean proportion of fruitlets (eight fruitlets from each of 6 biological replicate considered) showing GFP-labeled B05.10 growth on the selective media. Error bars indicate standard error. Mean proportions followed by a common letter within a dpi are significantly not different among NW, W and SS, according to Tukey's Honestly Significant Difference test ($P \leq 0.05$), using one way ANOVA. The mean proportions throughout the two weeks within NW, W or SS are not significantly different (ns).

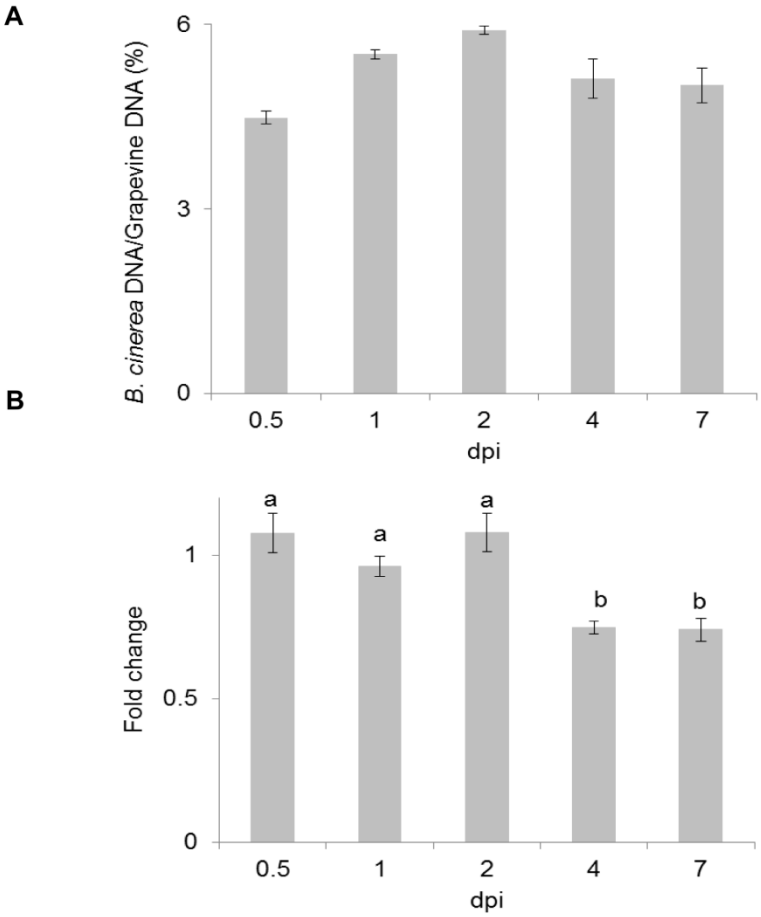

Figure 2. Relative quantification of genomic DNA (A) and expression profile of actin gene (B) from B. cinerea at different days post inoculation (dpi). A, Amount of *B. cinerea* gDNA relative to grapevine gDNA, measured by amplification of the *B. cinerea* gene *Bc3* (ribosomal IGS spacer) and the grapevine gene *VvRS I* (resveratrol synthase gene I) on gDNA from *Botrytis*-inoculated flowers. The Kruskal-Wallis one way ANOVA test revealed that the amount of *B. cinerea* gDNA at different dpi is not significantly different, P = 0.123. Error bar represents standard error of mean of three biological replicates. B, Relative expression of a *B. cinerea* actin gene, *BcACTA*, to monitor the growth of the pathogen in planta. Bars represent fold change of inoculated samples relative to PDB cultured *B. cinerea* (control). Normalization based on the expression levels of ribosomal protein L5, *BcRPL5*, and α tubulin, *BcTUBA*, was made before calculating fold changes. Expression values followed by the same letter are significantly not different between samples, according to Tukey's Honestly Significant Difference test ($P \leq 0.05$), using one way ANOVA on log2(NRQ).

Figure 2. Relative quantification of genomic DNA and expression profile of actin gene from *B*. *cinerea* at different days post inoculation (dpi). A, Amount of *B*. *cinerea* gDNA relative to grapevine gDNA, measured by amplification of the *B*. *cinerea* gene *Bc3* (ribosomal IGS spacer) and the grapevine gene *VvRS I* (resveratrol synthase gene I) on gDNA from *Botrytis*-inoculated flowers. The Kruskal-Wallis one way ANOVA test revealed that the amount of *B*. *cinerea* gDNA at different days post inoculation (dpi) is not significantly different, $P = 0.123$.

Error bar represents standard error of mean of three biological replicates. B, Relative expression of a *B*. *cinerea* actin gene, *BcACTA*, to monitor the growth of the pathogen *in planta*. Bars represent fold change of inoculated samples relative to PDB cultured *B*. *cinerea* (control). Normalization based on the expression levels of ribosomal protein L5, *BcRPL5*, and α tubulin, *BcTUB*A, was carried out before calculating fold changes. Expression values followed by the same letter are significantly not different between samples, according to Tukey's Honestly Significant Difference test ($P \leq 0.05$), using one way ANOVA on log2(NRQ).

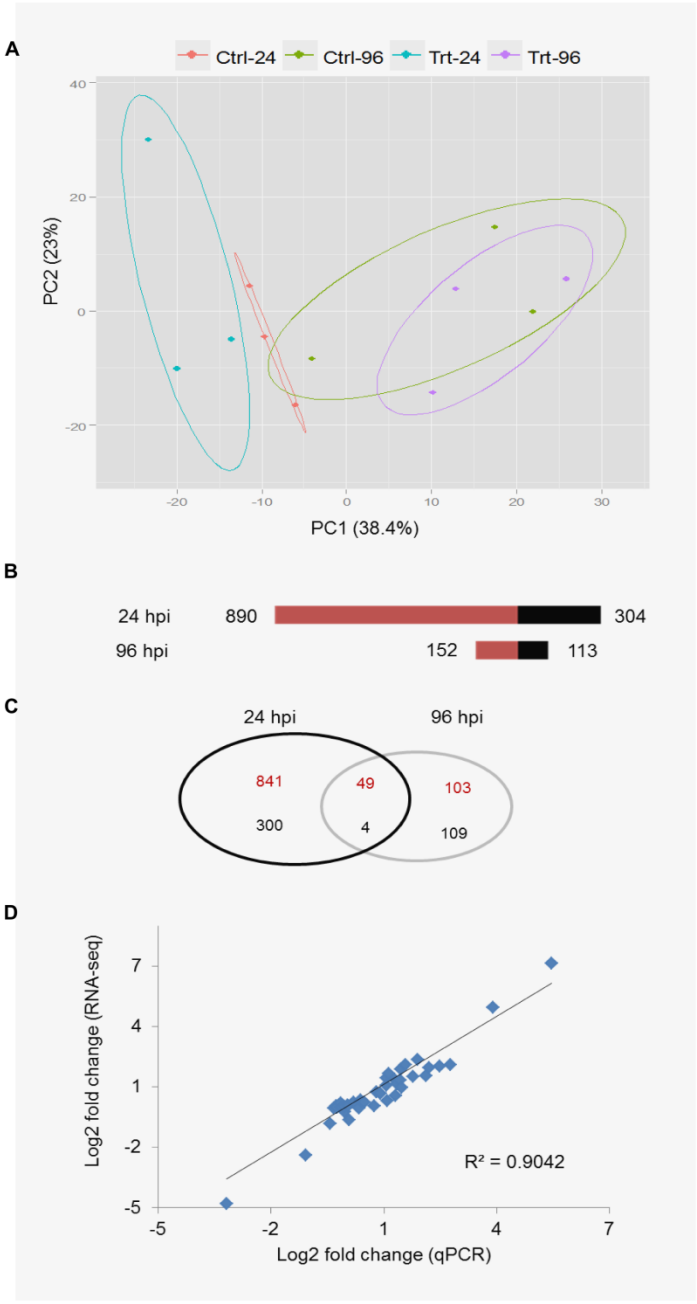

Figure 3. Analysis of the RNA-Seq data and of the differentially expressed (DE) genes. A, PCA displaying the biological variations among samples. Ctrl, mock inoculated; Trt, *B. cinerea* inoculated; Bc, *Botrytis cinerea*; 1-3 indicate the three biological replicates; 24 and 96 indicate hours post inoculation (hpi). Raw count data were used after precision weight was calculated by the voom method (Law et al., 2014). B, Number of DE genes ($P < 0.05$, fold change > 1.5) upon *B. cinerea* infection at 24 and 96 hpi; upregulated genes (red) and downregulated genes (black). C, Venn diagram showing the number of DE genes unique or common to 24 and 96 hpi. D, Validation of RNA-Seq data by qPCR assay: correlation of fold change values for 20 *Vitis* genes obtained by RNA-Seq and qPCR.

Figure 3. Analysis of the RNA-Seq data and of the differentially expressed (DE) genes. A, PCA displaying the biological variations among samples. Ctrl, mock inoculated; Trt, *B. cinerea* inoculated; Bc, *Botrytis cinerea;* 1-3 indicate the three biological replicates; 24 and 96 indicate hours post inoculation (hpi). Raw count data were used after precision weight was

calculated by the voom method (Law *et al*. 2014). B, Number of DE genes ($P < 0.05$, fold change > 1.5) upon *B*. *cinerea* infection at 24 and 96 hpi; upregulated genes (red) and downregulated genes (black). C, Venn diagram showing the number of DE genes unique or common to 24 and 96 hpi. D, Validation of RNA-Seq data by qPCR assay: correlation of fold change values for 20 *Vitis* genes obtained by RNA-Seq and qPCR.

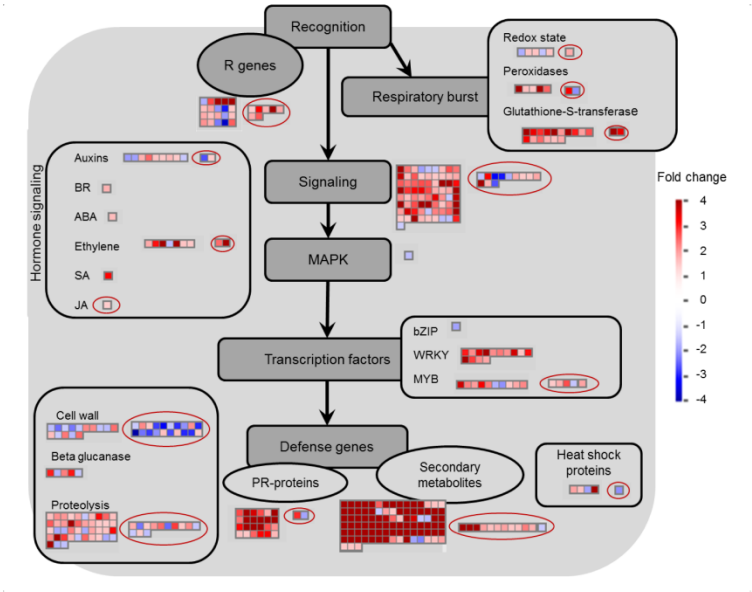

Figure 4. MapMan overview of biotic stress in inoculated flower at 24 and 96 hpi (red circled). Upregulated and downregulated genes are shown in red and blue, respectively. The scale bar displays fold change values. ABA, abscisic acid; BR, brassinosteroid; JA, jasmonic acid; MAPK, mitogen-activated protein kinase; SA, salicylic acid. The list of MapMan enriched pathways within DE genes is provided in Supporting Information Data S7.

b

Figure 4. MapMan overview of biotic stress in inoculated flower at 24 and 96 hpi (red circled). Upregulated and downregulated genes are shown in red and blue, respectively. The scale bar displays fold change values. ABA, abscisic acid; BR, brassinosteroid; JA, jasmonic acid; MAPK, mitogen-activated protein kinase; SA, salicylic acid. The list of MapMan enriched pathways within DE genes is provided in Supporting Information Data S7.

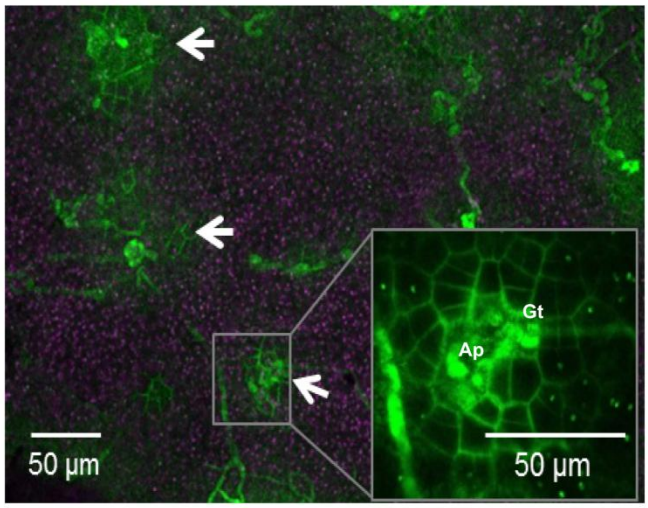

Figure 5. Confocal image of cytoplasmic HyPer grapevine transgenic flowers infected with *B. cinerea*. A higher intensity of HyPer fluorescence is evident 24 hpi at the penetration site of *B. cinerea*, compared with the rest of the plant tissue, indicating a localized and specific H_2O_2 accumulation (shown by arrows). The inset at higher magnification clearly shows that the bright signal comes from the cytosol of proximal cells to the site of infection.

Figure 5. Confocal image of cytoplasmic HyPer grapevine transgenic flowers infected with *B*. *cinerea*. A higher intensity of HyPer fluorescence is evident 24 hpi at the penetration site of *B*. *cinerea*, compared with the rest of the plant tissue, indicating a localized and specific H_2O_2 accumulation (shown by arrows). The inset at higher magnification clearly shows that the bright signal comes from the cytosol of proximal cells to the site of infection.

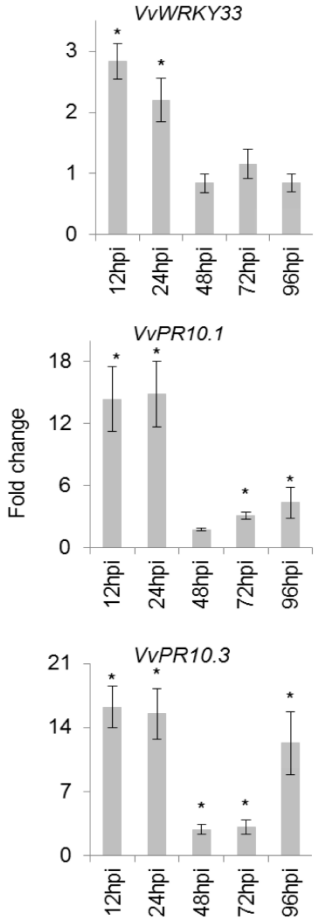

Figure 6. Expression profiles of VvWRKY33, VvPR10.1, and VvPR10.3 following *B. cinerea* inoculation. Gene expression levels were determined by qPCR. Bars represent fold change of inoculated sample relative to mock-inoculated sample at each post-inoculation time. Normalization based on the expression levels of actin, *VvACT* and tubulin, *VvTUB* was carried out before calculating fold changes. Error bar represents standard error of the mean of three biological replicates. Asterisks (*) indicate statistically significant difference ($P < 0.05$) between mock- and *B. cinerea*- inoculated samples within a post-inoculation time using unpaired heteroscedastic Student's t test. hpi, hours post inoculation.

Figure 6. Expression profiles of *VvWRKY33*, *VvPR10.1*, and *VvPR10.3* following *B. cinerea* inoculation. Gene expression levels were determined by qPCR. Bars represent fold change of inoculated sample relative to mock-inoculated sample at each post-inoculation time. Normalization based on the expression levels of actin, *VvACT* and tubulin, *VvTUB* was carried out before calculating fold changes. Error bar represents standard error of the mean of three biological replicates. Asterisks (*) indicate statistically significant difference ($P < 0.05$) between mock- and *B. cinerea*- inoculated samples within a post-inoculation time using unpaired heteroscedastic Student's t test. hpi, hours post inoculation.

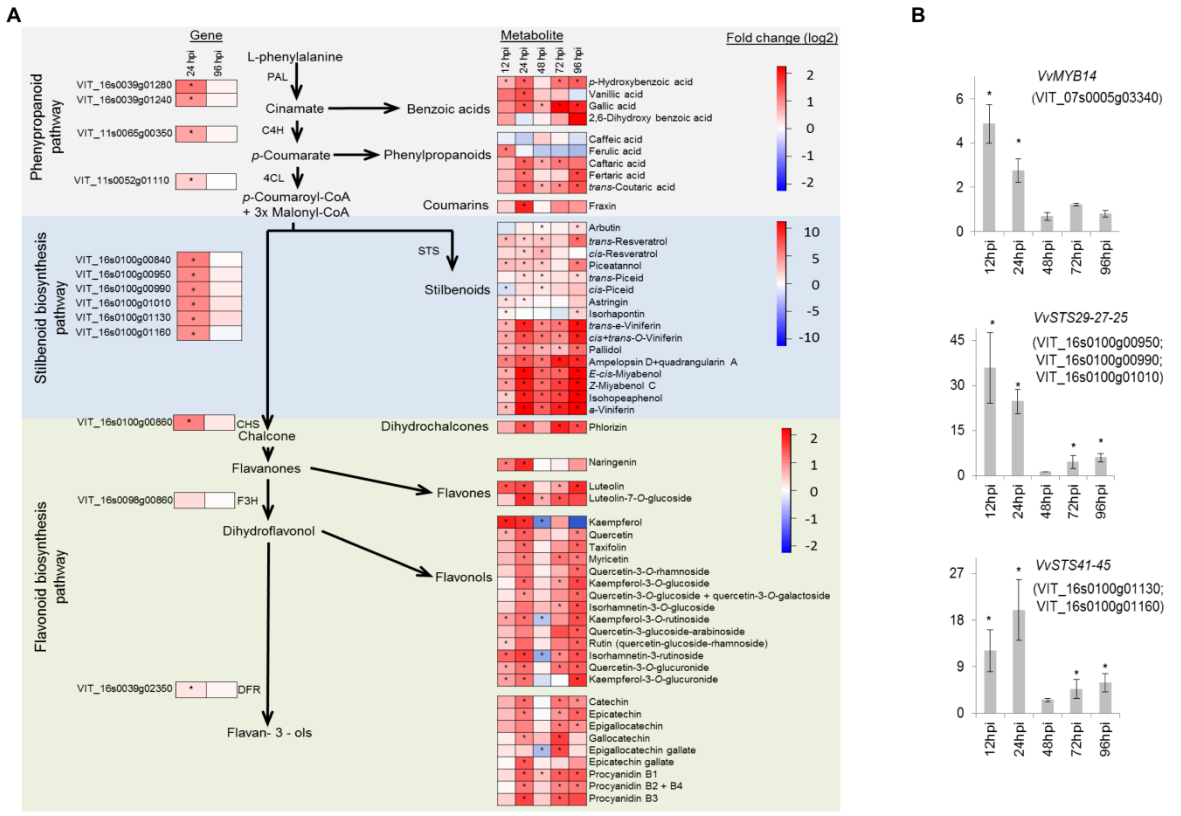

Figure 7. Transcript and metabolite analyses of the grapevine phenylpropanoid pathway upon *B. cinerea* inoculation. A, Heatmaps of gene expression (from RNA-Seq result) and secondary metabolite concentration (µg/g fw, from HPLC-DAAD-MS) expressed as fold change. Fold changes were computed based on the ratio of average values in *B. cinerea*- and mock-inoculated flowers, for each time point. CHS, chalcone synthase; C4H, cinnamate 4-hydroxylase; 4CL, 4-coumarate-CoA ligase; DFR, dihydroflavonol-4-reductase; F3H, flavanone 3-hydroxylase; PAL, phenylalanine ammonia lyase; STS, stilbene synthase (out of 39, only 6 are dipcted). B, Expression profile of *VvSTS29* (*-27-25*), *VvSTS41* (*-45*), and *VvMYB14*. Gene expression levels were determined by qPCR. Bars represent fold change of inoculated sample relative to mock-inoculated sample at each post-inoculation time. Normalization based on the expression levels of actin, *VvACT* and tubulin, *VvTUB* was carried out before calculating fold changes. Error bar represents standard error of the mean of three biological replicates. Asterisks (*) indicate statistically significant difference ($P < 0.05$) between mock- and *B. cinerea*-inoculated samples within a post-inoculation time using unpaired heteroscedastic Student's t test. hpi, hours post inoculation.

Figure 7. Transcript and metabolite analyses of the grapevine phenylpropanoid pathway upon *B*. *cinerea* inoculation. A, Heatmaps of gene expression (from RNA-Seq result) and secondary metabolite concentration (µg/g fw, from HPLC-DAAD-MS) expressed as fold change. Fold changes were computed based on the ratio of average values in *B*. *cinerea*- and mock-inoculated flowers, for each time point. CHS, chalcone synthase; C4H, cinnamate 4-hydroxylase; 4CL, 4-coumarate-CoA ligase; DFR, dihydroflavonol-4-reductase; F3H, flavanone 3-hydroxylase; PAL, phenylalanine ammonia lyase; STS, stilbene synthase (out of 39, only 6 are dipcted). B, Expression profile of *VvSTS29* (*-27-25*), *VvSTS41* (*-45*), and *VvMYB14*. Gene expression levels were determined by qPCR. Bars represent fold change of inoculated sample relative to mock-inoculated sample at each post-inoculation time. Normalization based on the expression levels of actin, *VvACT* and tubulin, *VvTUB* was

carried out before calculating fold changes. Error bar represents standard error of the mean of three biological replicates. Asterisks (*) indicate statistically significant difference ($P < 0.05$) between mock- and *B*. *cinerea*-inoculated samples within a post-inoculation time using unpaired heteroscedastic Student's t test. hpi, hours post inoculation.

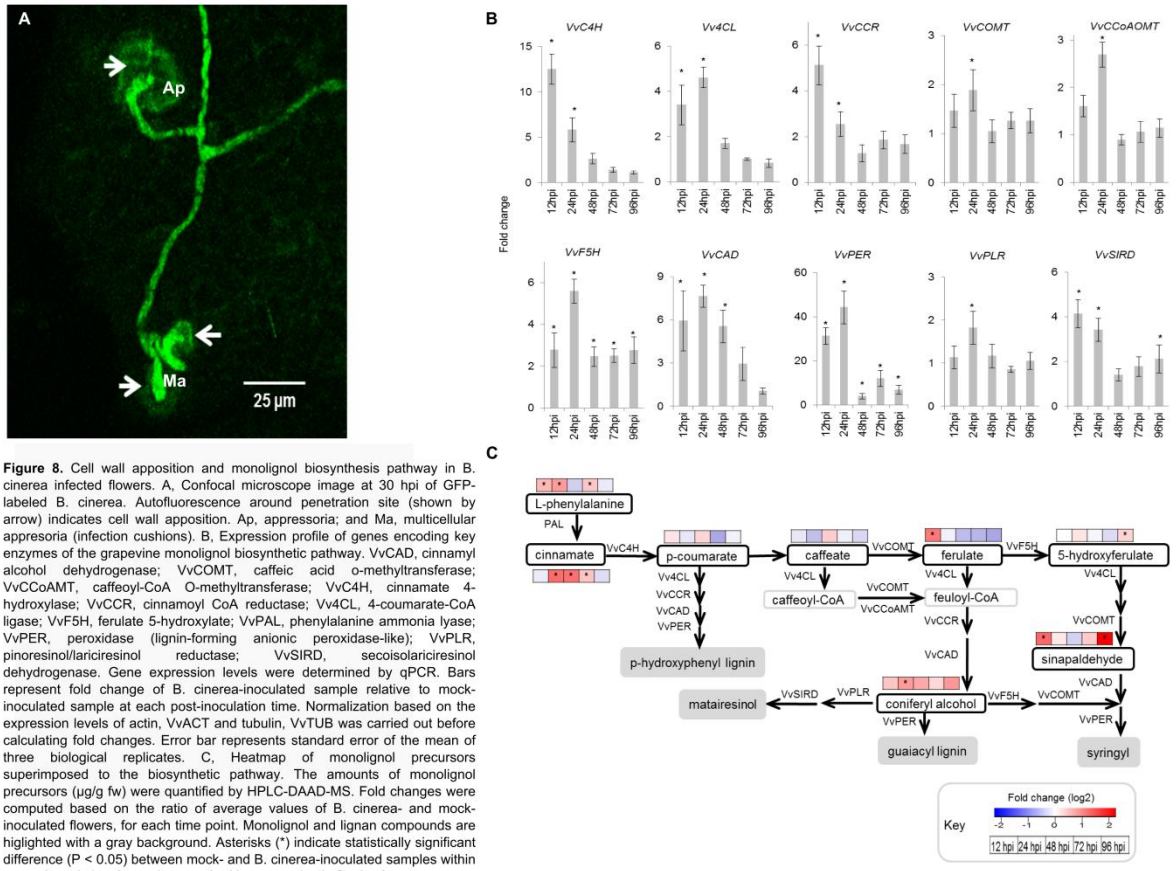

Figure 8. Cell wall apposition and monolignol biosynthesis pathway in B. cinerea infected flowers. A, Confocal microscope image at 30 hpi of GFP-labeled B. cinerea. Autofluorescence around penetration site (shown by arrow) indicates cell wall apposition. Ap, appressoria; and Ma, multicellular appresoria (infection cushions). B, Expression profile of genes encoding key enzymes of the grapevine monolignol biosynthetic pathway. VvCAD, cinnamyl alcohol dehydrogenase; VvCOMT, caffeic acid o-methyltransferase; VvCCoAMT, caffeoyl-CoA O-methyltransferase; VvC4H, cinnamate 4-hydroxylase; VvCCR, cinnamoyl CoA reductase; Vv4CL, 4-coumarate-CoA ligase; VvF5H, ferulate 5-hydroxylate; VvPAL, phenylalanine ammonia lyase; VvPER, peroxidase (lignin-forming anionic peroxidase-like); VvPLR, pinoresinol/lariciresinol reductase; VvSIRD, secoisolariciresinol dehydrogenase. Gene expression levels were determined by qPCR. Bars represent fold change of B. cinerea-inoculated sample relative to mock-inoculated sample at each post-inoculation time. Normalization based on the expression levels of actin, VvACT and tubulin, VvTUB was carried out before calculating fold changes. Error bar represents standard error of the mean of three biological replicates. C, Heatmap of monolignol precursors superimposed to the biosynthetic pathway. The amounts of monolignol precursors (µg/g fw) were quantified by HPLC-DAAD-MS. Fold changes were computed based on the ratio of average values of B. cinerea- and mock-inoculated flowers, for each time point. Monolignol and lignan compounds are higlighted with a gray background. Asterisks (*) indicate statistically significant difference ($P < 0.05$) between mock- and B. cinerea-inoculated samples within a post-inoculation time using unpaired heteroscedastic Student's t test.

Figure 8. Cell wall apposition and monolignol biosynthesis pathway in *B. cinerea* infected flowers. A, Confocal microscope image at 30 hpi of GFP-labeled *B. cinerea*. Autofluorescence around penetration site (shown by arrow) indicates cell wall apposition. Ap, appressoria; and Ma, multicellular appresoria (infection cushions). B, Expression profile of genes encoding key enzymes of the grapevine monolignol biosynthetic pathway. *VvCAD*, cinnamyl alcohol dehydrogenase; *VvCOMT*, caffeic acid o-methyltransferase; *VvCCoAMT*, caffeoyl-CoA O-methyltransferase; *VvC4H*, cinnamate 4-hydroxylase; *VvCCR*, cinnamoyl CoA reductase; *Vv4CL*, 4-coumarate-CoA ligase; *VvF5H*, ferulate 5-hydroxylate; *PAL*, phenylalanine ammonia lyase; *VvPER*, peroxidase (lignin-forming anionic peroxidase-like); *VvPLR*, pinoresinol/lariciresinol reductase; *VvSIRD*, secoisolariciresinol dehydrogenase. Gene expression levels were determined by qPCR. Bars represent fold change of *B. cinerea*-inoculated sample relative to mock-inoculated sample at each post-inoculation time.

Normalization based on the expression levels of actin, *VvACT* and tubulin, *VvTUB* was carried out before calculating fold changes. Error bar represents standard error of the mean of three biological replicates. C, Heatmap of monolignol precursors superimposed to the biosynthetic pathway. The amounts of monolignol precursors (µg/g fw) were quantified by HPLC-DAAD-MS. Fold changes were computed based on the ratio of average values of *B. cinerea*- and mock-inoculated flowers, for each time point. Monolignol and lignan compounds are highlighted in gray background. Asterisks (*) indicate statistically significant difference ($P < 0.05$) between mock- and *B. cinerea*-inoculated samples within a post-inoculation time using unpaired heteroscedastic Student's t test.

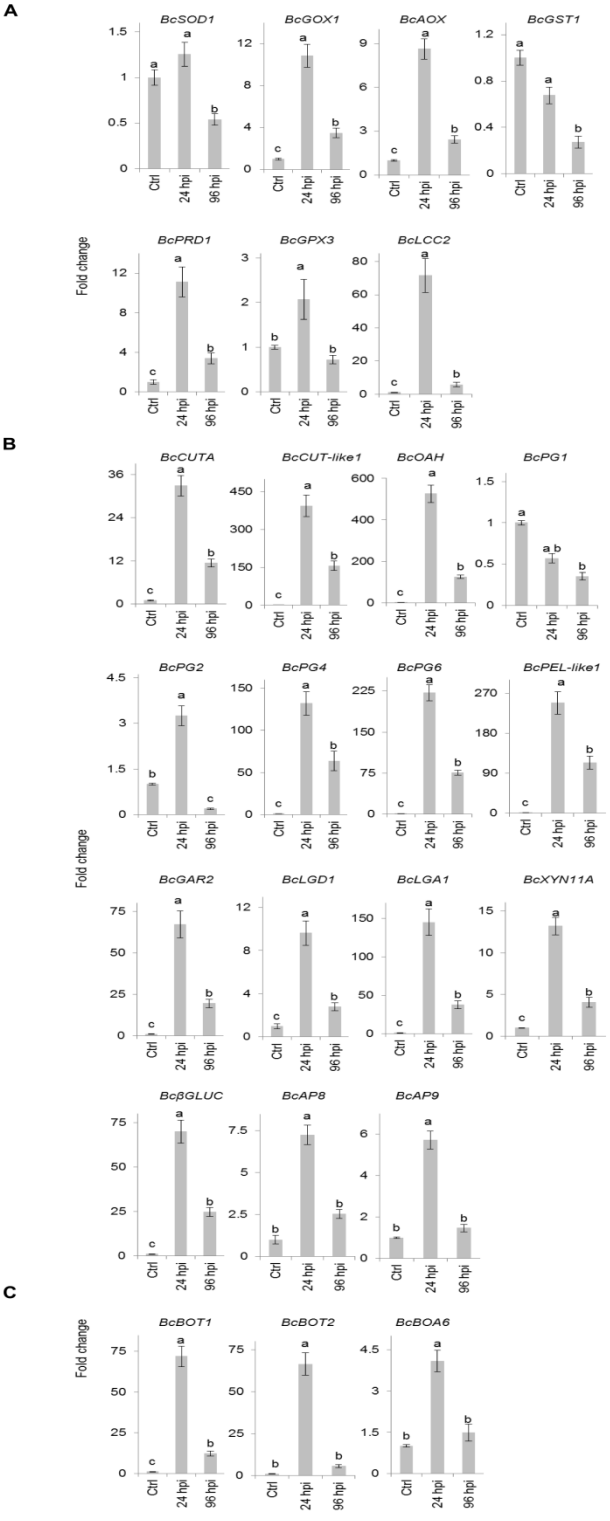

Figure 9. Expression profile of growth- and virulence-related *Botrytis cinerea* genes during grapevine flower infection (at 24 and 96 hpi) relative to PDB-cultured *B. cinerea*. A, Reduction-oxidation related genes. B, Cell wall degrading enzymes and proteases encoding genes. C, Phytotoxin encoding genes. Gene expression levels were determined by qPCR. Bars represent fold change of sample at 24 or 96 hpi relative to the PDB-cultured *B. cinerea* (Ctrl). Normalization based on the expression levels of ribosomal protein L5, *BcRPL5*, and α tubulin, *BcTUBA*, was carried out before calculating fold changes. Error bar represents standard error of the mean of three biological replicates. Expression values followed by a common letter are significantly not different between samples, according to Tukey's Honestly Significant Difference test ($P \leq 0.05$), using one way ANOVA of log2 (NRQ).

Figure 9. Expression profile of growth- and virulence-related *Botrytis cinerea* genes during grapevine flower infection (at 24 and 96 hpi) relative to PDB-cultured *B*. *cinerea*. A, Reduction-oxidation related genes. B, Cell wall degrading enzymes and proteases encoding genes. C, Phytotoxin encoding genes. Gene expression levels were determined by qPCR. Bars represent fold change of sample at 24 or 96 hpi relative to the PDB-cultured *B*. *cinerea* (Ctrl). Normalization based on the expression levels of ribosomal protein L5, *BcRPL5*, and α tubulin, *BcTUBA*, was carried out before calculating fold changes. Error bar represents standard error of the mean of three biological replicates. Expression values followed by a common letter are significantly not different between samples, according to Tukey's Honestly Significant Difference test ($P \leq 0.05$), using one way ANOVA of log2(NRQ).